Bioprinting and *In Vitro* Characterization of an Egg White-Based Cardiac Patch for Myocardial Infarction

A Thesis Submitted to the College of
Graduate Studies and Research
In Partial Fulfillment of the Requirements
For the Degree of Master of Science
In the Division of Biomedical Engineering
University of Saskatchewan
Saskatoon, Saskatchewan
Canada

By
Yasaman Delkash

Permission to Use

In presenting this thesis in partial fulfillment of the requirements for a Master of Science degree from the University of Saskatchewan, I agree that the Libraries of this University may make it freely available for inspection. I further agree that permission for copying of this thesis in any manner, in whole or in part, for scholarly purposes, may be granted by the professor or professors who supervised my thesis work or, in their absence, by the Head of the Department or the Dean of the College in which my thesis work was done. It is understood that any copying or publication or use of this thesis or parts thereof for financial gain shall not be allowed without my written permission. It is also understood that due recognition shall be given to me and to the University of Saskatchewan in any scholarly use which may be made of any material in my thesis.

Requests for permission to copy or to make other uses of materials in this thesis/dissertation in whole or part should be addressed to:

Dean
College of Graduate and Postdoctoral Studies
University of Saskatchewan
116 Thorvaldson Building, 110 Science Place
Saskatoon, Saskatchewan S7N 5C9
Canada

or

Head of the Division of Biomedical Engineering
57 Campus Drive, University of Saskatchewan
Saskatoon, Saskatchewan S7N 5A9
Canada

Abstract

Myocardial infarction (MI) or heart attack occurs when the bloodstream to the heart is blocked, which may destroy a part of the heart muscle (or myocardium) and form perdurable scarred tissue. The infarcted myocardial muscle nowadays has no revival treatments, and also transplantation is limited as an option. Tissue engineering has the potential to restore myocardial function after an MI by fabricating tailored tissues for treatment. For tissue engineering, three-dimensional (3D) bioprinting is a fabrication method to create 3D constructs with living cells, which would be impossible by other traditional methods. Although various biomaterials, biologically-derived or synthetic, are available, only a few can be used in 3D bioprinting of cardiovascular tissues due to their mechanical weakness of natural biomaterials and/or limited bioactivity (in terms of promoting cell functions) of synthetic ones. The present study aims to develop a novel biomaterial solution for bioprinting (referred to as bioink) and on this basis, to bioprint cell-laden patches and characterize the patches *in vitro* for potential use in MI treatment.

For this, a new bioink was formulated based on chicken egg white (EW) and sodium alginate (Alg). EW, as a rich source of albumin and well-known for its drug delivery applications, has been strategically combined with Alg, a common printable polysaccharide with a non-thrombogenic nature. EW was utilized to improve bioactivity and cell adhesion sites and sodium alginate was considered as an extrudability enhancer to provide good printability. The following research objectives were pursued: I) develop and rheologically characterize the albumin-based bioink by adding minimal amounts of alginate as a printability enhancer biomaterial; II) characterize the mechanical properties of the 3D printed albumin-based patches by compression testing and monitoring the swelling and degradation behavior; and III) characterize the biological properties of the 3D bioprinted cell-laden albumin-based patch by examining the *in vitro* cell viability.

EW-Alg blends with different alginate concentrations were synthesized by mixing the pasteurized egg white with sodium alginate powder. Then the blends were tested in terms of their rheological behavior and showed a non-Newtonian shear-thinning functioning, i.e. the increase of shear strain led to a decline in viscosity. Moreover, the addition of each 0.5 gram alginate in 100 milliliter egg white significantly consolidated the blend's texture and notably changed its viscosity

and handling. Hence, the more alginate was used in the solution, the higher the blend's viscosity and the required extrusion pressure.

Compression elastic moduli of the 3D printed patches from the printable EW-Alg blends (2.0, 2.5, and 3.0% Alg in EW) with the range 20-27 kPa showed the similarity of these constructs mostly to human cadaver limb specimens with 10-38 kPa compressive elastic modulus. Furthermore, swelling measurements performed in phosphate-buffered saline (PBS) showed swelling ratios of more than 1800% for all three concentrations of the EW-Alg blend, representing these 3D printed patches' ability to uptaking ionic fluids from a body-like environment. Also, all of the constructs showed signs of biodegradation within a month.

The EW-2.0%Alg blend, which had the highest egg white ratio to alginate and the lowest viscosity, was 3D bioprinted as a cell-laden bioink. The loaded human umbilical vein endothelial cells (HUVECs) survival rate was more than 90% in all of the time points within a week, showing high biocompatibility of the EW-Alg bioink.

The present study developed an egg white-based bioink for 3D cardiac patch bioprinting. Fabricated patches exhibited suitable mechanical properties and biocompatibility *in vitro*, to be potentially used for MI treatment.

Acknowledgments

I would like to express my gratitude to my supervisors, Dr. Daniel Chen and Dr. Sean Maw who gave me the golden opportunity to do this informative thesis and kindly supported me through all this work.

I also extend my appreciation to my thesis advisory committee, Dr. W.J. (Chris) Zhang, and Dr. Michael Kelly, for their valuable advice and suggestions towards completing this MSc. thesis.

My sincere thanks also go to Dr. Petros Papagerakis for providing the lab facility regarding the cell study part of this thesis, and his Ph.D. student Fatemeh Mohabbatpour for the related training.

I also thank our group's undergraduate visiting students, Maxence Gouin, and Tanguy Rimbeault, from ICAM University, France, for their practical help, and the rest of my lab mates for the all the great moments we have had in the last two years.

I would like to express my special thanks to my caring, loving, and supportive husband, Arash Nemati for his heartwarming support.

The financial support of this study from the Natural Science and Engineering Research Council (NSERC) of Canada is acknowledged.

Table of Contents

List of Abbreviations

2D: two-dimensional
3D: three-dimensional
Alg: alginate
ANOVA: analysis of variance
BCPs: biphasic calcium phosphates
bFGF: basic fibroblast growth factor
CAD: computer-aided design
$CaCl_2$: calcium chloride
CMs: cardiomyocytes
CNT: carbon nanotubes
CO_2: carbon dioxide
CPCs: cardiac progenitor cells
CSCs: cardiac stem cells
DMEM: Dulbecco's Modified Eagle's Medium
(d)ECM: (decellularized) extracellular matrix
ESC: endothelial stem cells
EW: egg white
FBS: fetal bovine serum
FDA: Food and Drug Administration
FRESH: freeform reversible embedding of suspended hydrogels
GAG: glycosaminoglycan
GelMA: gelatin methacrylate
HAGM: hyaluronic acid glycidyl methacrylate
hMSCs: human mesenchymal stem cells
hESCs: human embryonic stem cells
HUVEC: human umbilical vein endothelial cell
IGF-1: insulin-like growth factor 1
iPSC: induced pluripotent stem cell
LV: left ventricular
MA: methacrylate
MI: myocardial infarction
NRVM: neonatal rat ventricular myocytes
NSCs: neural stem cells
PCL: poly (ε-caprolactone)
PBS: phosphate-buffered saline
PDGF-β: Platelet-derived growth factor subunit β
PEG: poly (ethylene glycol)

PEI: poly (ethylenimine)
PGS: poly(glycerol sebacate)
pHEMA: poly (2-hydroxyethyl methacrylate)
PLLA: poly (L) lactide
RGD: arginine-glycine-asparagine or Arg-Gly-Asp
SDF-1: stromal cell-derived factor 1
SEM: scanning electron microscopy
SIS: small intestinal submucosa
UV: ultraviolet
VEGF: vascular endothelial growth factor
μCOP: micro-continuous optical printing

List of Figures

List of tables

Chapter 1: Introduction

1.1 Myocardial Infarction

Heart attack or myocardial infarction (MI) occurs when one or multiple heart coronary arteries are disabled to deliver the blood to the heart, causing irreversible damage to the heart muscle [1]. In contrast with other organs, heart muscle regeneration is almost absent in adulthood since the cardiomyocyte differentiation is almost terminated [2].

A variety of cardiovascular diseases and disorders can lead to MI (such as the formation of blood clots, coronary diseases, and neurological disorders), and MI continues to be a deadly problem globally each year [3]. Current solutions include different surgeries to remove the obstruction that had led to the occurred infarction or compensating for the infarcted myocardium's function. Coronary bypass surgery, angioplasty, stenting, implanting pacemakers or defibrillators, and valve replacement are some of the conventional proceedings [4]. Also, in the acute cases where the infarcted area is large and heart failure is in the end-stage, heart transplantation is needed. However, the number of donations has never been enough, and also the risk of the rejection of the donor's heart exists.

1.2 Cardiac Tissue Engineering

Lack of curing methods that can reverse the scarred heart muscle and restore its function have increased the tissue engineering research demands to develop new treatments with regenerative capacity.

The first 3D cardiac structure was constructed by Moscona et al. in 1952 [5]. In 1959, this group generated spheroid aggregates from embryonic chicken heart cells. They cultivated freshly isolated cells in Erlenmeyer flasks under continuous gyration [6]. Since then, different heart tissue engineering approaches such as cell transplantation, injectable scaffolds, and myocardial patches have been developed to help repair the damaged site [7]. The purpose is engineering the infarcted region for healing and restoration of its innate function.

In the cell transplantation method, a suspension of cells that usually contains stem cells or progenitor cells is injected directly or indirectly into the infarcted area for further repopulation of

the cardiac cells within the scarred region [8]. The main challenge here is the transplanted cells' low survival rate due to various reasons such as inflammation, fibrosis, and/or shortage of blood supply [9]. The lack of extracellular matrix (ECM) support in this method plays a critical role in cell fate and survival due to the deprivation of environmental signaling and transportation, which are normally provided by ECM [10].

Injectable hydrogels may be an approach to solicit ECM support. This approach is an in-situ reconstruction of the tissue. Injectable structures, usually made of water-soluble biomaterials, are combined with necessary biological factors for regeneration, such as growth factors or cells (like stem cells), and directly are injected into the infarcted area of the heart [11][12]. This method, although less invasive than implanting *in vitro* engineered tissues, has some disadvantages. The presence of the crosslinking agents inside the body and unreacted particles creates a risk of further toxicity problems [13]. Also, the size, shape, and development of the engineered construct are not entirely controllable. Besides, similar to the cell transplantation approach, the cell survival rate is low because of the surgical stress cells incur during the injection process [7].

In vitro made cardiac patches are the other tissue engineering approach in which an implantable construct (or patch) provides physical and biochemical cues for myocardium regeneration. These engineered patches can be generally classified into two main groups called 2D cell sheets and 3D cell-laden patches [14]. In the cell sheet method, myocardial cells are cultured in a dish and are connected by cell junctions. Usually, the culture dish button is covered by a temperature-sensitive polymer such as poly N-isopropyl acrylamide (PIPAAm) to facilitate detaching the cell sheet from the plate by changing the temperature [15]. Single-layer sheets can then be assembled on top of each other to make 3D cardiac constructs. This layered structure arranges well-aligned cells that are required for the proper pulsation feature in cardiac tissue. This approach has some challenges as the number of layers of the construct increases. For example, weak electrical and morphological communications, plus inadequate perfusion of growth factors and biological agents among the layers, are common problems in this method due to lack of a suitable network system [14].

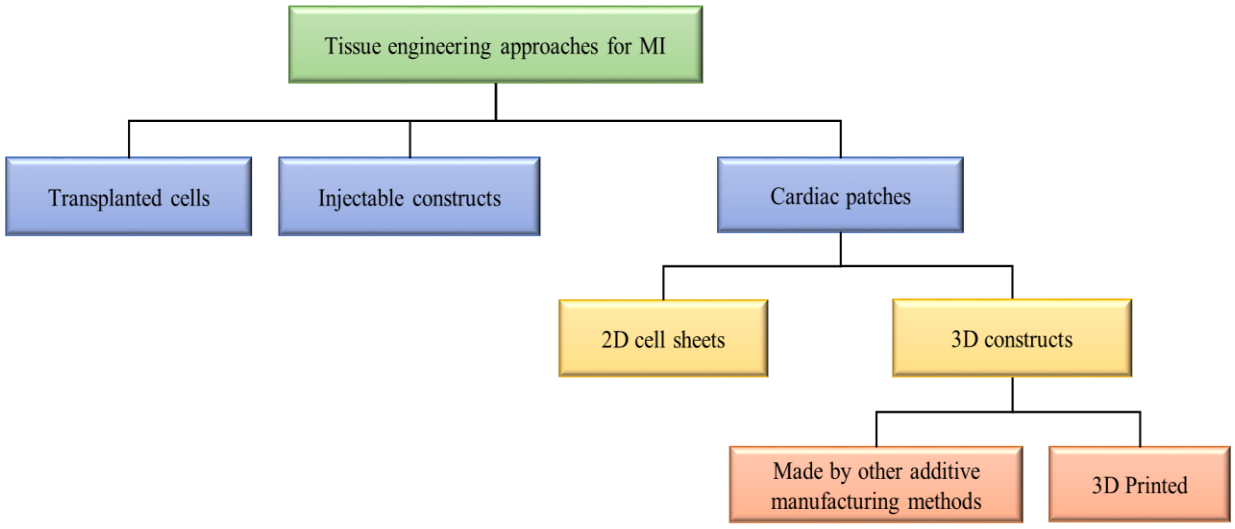

Figure 1-1 Overview of tissue engineering solutions for MI

An alternative approach is 3D porous interconnected patches in which cells are suspended in a matrix of biomaterial. This design gives us more freedom to gather desirable features, such as employing a combination of fabrication methods, cell types, and biomaterials. 3D printing and electrospinning are two conventional methods for the fabrication of 3D architectures. These methods enable tailoring patch properties via optimization of the materials and processing parameters [16]. This control can have subsequent roles in the manipulation of cell behavior for tissue engineering [16].

Electrospun constructs often have random architectures, whereas, in 3D printing, 3D models are built in a computer-controlled layer-by-layer process. Such an organized design empowers the integration of more complicated features like vasculature networks owing to having control over the patch's architecture [17][18]. In 3D printing, cells can be incorporated into biomaterials and pattern thick tissue living constructs that could not be formed using other fabrication methods [19]. Using this method can result in porous constructs (or matrices) with specific shapes and dimensions that subsequently might affect initial adhesion, proliferation, and differentiation of the cultured cells in the presence of corresponding bioactive components such as growth factors and enzymes [20]. This technology gives us the hope of fabricating patches with similar morphology and accuracy to the native ECM [21].

1.3 Extrusion-Based 3D Printing

Extrusion-based 3D printing is an additive manufacturing methodology in which materials are selectively dispensed through a nozzle (or dispenser) layer by layer. In this method, using computer-aided design (CAD) software, the desired 3D construct model is created. By this design and by optimizing the printing parameters, control over the pore size, pore geometry, and spatial distribution of pores is possible [22].

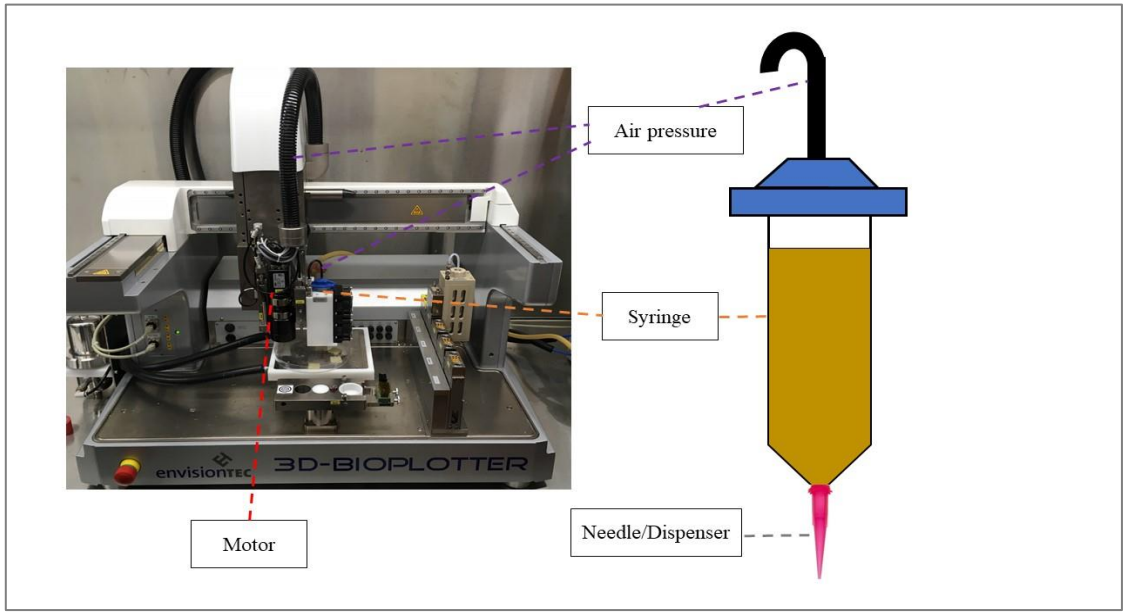

Figure 1-2 Extrusion based 3D bioplotter compartments

Extrusion-based 3D printing is the most common type of 3D printing in terms of various choices for materials, precision in printing complex structures, ease of operation, adaptability with many environments, and diversity of solidification approaches [23]. Using this tissue engineering fabrication technique also provides direct cell incorporation into the printing biomaterials [22][24]. Many cardiac tissue-like constructs have been printed by this method, showing successful results *in vivo*. These constructs will be discussed later in Chapter 2.

1.4 Research Objectives

The present study aims to develop an albumin-based bioink and on this basis, bioprint and characterize cell-laden patches for potential use in MI treatment. To accomplish this aim, the following investigations are set to be conducted.

1) Develop and rheologically characterize the albumin-based bioink by adding minimal amounts of alginate for improved printability.
2) Characterize the mechanical properties of the 3D printed albumin-based patches by compression testing as well as swelling and degradation behavior.
3) Characterize the biological properties of the 3D bioprinted cell-laden albumin-based patch by *in vitro* cell viability assessment.

1.5 Thesis Outline

This thesis contains six chapters. **In Chapter 1**, MI is introduced as a life-threatening cardiovascular disease. Tissue engineering, as a potential treatment, and various tissue fabrication methods, especially extrusion-based 3D bioprinting, are discussed. Also, the research objectives of the present study are stated in this chapter. **In Chapter 2**, common printing biomaterials and bioinks, studied in the literature for the 3D (bio)printing of a cardiac patch, are examined followed by key strategies relevant to this area. Accordingly, EW is introduced as a potential beneficial bioink for cardiac patch 3D bioprinting. **Chapter 3** presents the EW-Alg inks' preparation method, along with rheological assessments and 3D printing of these potential bioinks. **In Chapter 4**, compression elastic modulus, swelling ability, and degradation behavior, as mechanical properties of the 3D printed EW-Alg constructs, are investigated. **In Chapter 5**, the cell viability within the bioprinted HUVECs-laden cardiac patch made of EW-Alg is tested as an *in vitro* biological characterization. **Chapter 6** summarizes the present study, the conclusions drawn, and the recommendations suggested for future work.

Chapter 2: Literature Review

2.1 Introduction

This chapter reviews the biomaterials and strategies used in 3D (bio)printing of cardiovascular tissues, particularly for cardiac patches. Egg white (EW) with a remarkable range of biomedical applications is proposed later as a potential bioink for 3D bioprinting a cardiac patch. Bioink is defined as the material using in tissue 3D printing when it contains cells or biological compartments [22].

2.2 Bioinks and Printing Biomaterials for Cardiac Patches

Biocompatibility and printability are two desired features for material as a bioink in 3D (bio)printing. Most biomaterials used as bioink are derived from natural extracellular matrix sources [22]. However, synthetic materials have their own advantages, such as providing better mechanical support for the construct [25]. Here, natural and synthetic biomaterials used frequently in 3D printing of cardiovascular constructs are reviewed.

2.3 Natural Biomaterials

Natural cardiac bioinks include ECM-derived proteins and glycosaminoglycans (e.g. collagen), decellularized intact ECM or dECM (e.g. small intestine submucosa), materials derived from plants (e.g. cellulose), seaweed (e.g. alginate), and crustaceans (e.g. chitosan) [23]. The most commonly used natural materials for constructing cardiac patches via 3D (bio)printing methods are reviewed in this section.

2.3.1 Decellularized extracellular matrix (dECM)

dECM has the advantage of containing a physiological proportion of the native tissue components, such as the structural proteins fibronectin, collagen, laminin, glycosaminoglycans (GAGs) and growth factors [26]. In the case of cardiac tissue engineering, dECM can be derived from either cardiac sources, such as myocardium [27] and pericardium [28], or non-cardiac sources

like small intestinal submucosa (SIS) [29] and urinary bladder matrix [30]. However, preparing this material for tissue engineering applications needs processing, which generally takes place in 3 steps:

1) obtaining ECM from tissue specimens or using *in vitro* sheets created by cell culture;

2) using a decellularization process;

3) recellularizing the ECM with the desired cell type [16].

On the other hand, pure ECM can be challenging to use due to its soft mechanical properties and handling difficulties [31]. Extrusion bioprinting has attempted to overcome these problems through condensing ECM, using crosslinking modifications, and combining dECM with other biomaterials [32]. Such bioinks, combined with cells, have been proposed for cardiac tissue engineering in different studies [31][33]. For example, in the Bejleri et al. study, porcine cardiac ECM combined with gelatin methacrylate (GelMA), which provided a high degree of printability and proper mechanical properties for constructs, was used as the bioink of a 3D cardiac patch. This ECM-GelMA bioink was loaded with human cardiac progenitor cells (hCPCs), which resulted in the high maintainability of these cells (>75% viability), in addition to a 30-fold increase in their cardiogenic gene expression [34]. This ECM-GelMA-hCPCs patch also increased angiogenic potential (>2-fold) over the patch made of GelMA alone, by promoting endothelial cell tube formation.

In another study, having dECM as bioink improved the bioactivity and cell survival of the construct. Endothelial induction of MSCs and enhanced functionality of hCPCs were also a result of the presence of a 3D printed patch composed of cardiac ECM containing vascular endothelial growth factor (VEGF) [35]. The developed patch also promoted remarkable vascularization and tissue matrix formation *in vivo*. The patch's 3D pattern led to enhanced cardiac functions, reduced cardiac hypertrophy and fibrosis, and increased migration from patch to the infarcted area. Neo-muscle and capillary formation were also improved along with cardiac functions. This patch provided a cardiac niche-like microenvironment, resulting in positive effects on cardiac repair [35][32].

2.3.2 Collagen

Collagen is one of the major components of natural ECM in adult heart tissue that promotes cardiomyocytes' growth and survival [26]. On the other hand, it has poor mechanical properties,

which makes it difficult to process. Therefore, collagen is usually used in combination with other natural or synthetic materials [36]. For example, in the Duan et al. study, collagen type I combined with porcine cardiac dECM in various ratios was examined to differentiate human embryonic stem cells (hESCs) into cardiomyocytes [26]. These hybrid hydrogels improved the contractile function of cardiac cells in addition to the cardiomyogenic gene expression in the applied stem cells.

Another way to enhance collagen's mechanical properties to make it suitable for printing is by crosslinking it with different methods such as irradiation and thermal polymerization [22] while its biological features remain intact. Crosslinkable collagen injected into a rat model with ischemia-reperfusion has led to angiogenesis improvements by increasing the capillarity density [37].

Collagen might be able to be printed more easily by other methods of 3D printing. Freeform reversible embedding of suspended hydrogels (FRESH) is one of the 3D bioprinting techniques in which the material is extruded into a supportive hydrogel bath. This bath maintains the intended structure during the printing process and significantly improves print fidelity [38]. Collagen has been printed using the FRESH technique to generate human coronary vessels and trabeculated embryonic heart [39]. For example, a fibrinogen-collagen-Matrigel bioink containing C2C12 myoblasts and MC3T3 fibroblasts was FRESH-printed with 99.7% post-printing cell viability. This study revealed that printed cells formed dense cellular networks over time in culture [26].

The most popular types of collagen for cardiovascular tissue engineering applications are collagens type I and III due to their functional role in blood vessel structure and cardiac ECM [40]. However, type I is the thicker fibrillary collagen with more rigidity and stability [41], which might make it a more suitable type for machining to build 3D bioprinted patches.

2.3.3 Gelatin

Gelatin is denatured collagen after heating. It is one of the commonly used materials in 3D printed structures with excellent printability [23]. Tijore et al. have printed gelatin hydrogels in a micro-channel pattern to promote myocardial differentiation of the human mesenchymal stem cell (hMSC) [42]. This pattern was also effective on native cardiomyocytes' (CMs) contractile functionality. However, gelatin is challenging in 3D printing because of its thermosensitivity. Also, it melts rapidly at 37 ˚C. As a solution, combining gelatin with methacrylate can make a new hydrogel called gelatin methacrylate (GelMA). GelMA is crosslinkable by UV light, and this helps

the stability of the printed construct. It has remarkable bioactivity similar to gelatin, and enhanced mechanical properties which is due to its photo-crosslinked structure. GelMA has also been used in engineering tissue analogs ranging from the vasculature to cartilage and bone [43]. GelMA bioink enriched with fibronectin has shown supporting cell survival and spreading of the cardiomyocytes within 3D heart tissue constructs [44].

Gelatin has also been combined with other natural materials such as hyaluronic acid and alginate to optimize the patches' biological and physicochemical properties [45][46]. For example, in a recent study, GelMA combined with hyaluronic acid was used as the bioink for a light-based micro-continuous optical printing (μCOP) device to construct a human cardiac model [47]. In that study, researchers printed a cantilever system made of GelMA and hyaluronic acid glycidyl methacrylate (HAGM), which contained human embryonic stem cell-derived cardiomyocytes (hESC-CMs). Pairing the green fluorescent protein calmodulin/M13 peptide (GCaMP) calcium sensor with the printed materials helped monitor cell viability and alignment [47]. Such functional cardiac constructs can also help various biomedical and clinical tests such as drug discovery and biosafety.

2.3.4 Fibrin

Fibrin, an FDA-approved natural biopolymer for many medical applications, has competent biocompatibility and non-inflammatory properties [48]. Fibrin is obtained by mixing fibrinogen monomers with thrombin in saline solution. In this process, a 3D net is formed after polymerization, which is similar to normal clotting mechanisms *in vivo*. Properties of this network are tailorable by modifying the polymerization process [49].

Fibrin has a crucial role in wound healing and blood clotting. As a result, it has an extensive application in skin and wound repair research [50]. It is also popular in cardiovascular tissue engineering [51]. Fibrin improves the healing process and has a protective effect against myocardial reperfusion injury because it contains arginine-glycine-asparagine (RGD), promoting cell adhesions [52]. Besides, fibrin’s positive effect on differentiating the bone marrow stem cells into cardiomyocytes has been observed in studies [53]. Fibrin’s source can be the patient’s blood. This possibility enables fibrin to act as an autologous scaffold for tissue engineering [54].

Fibrin has been used in cardiac construct studies as a bioink in incorporating synthetic materials, which can improve the structure's mechanical properties. In one study, fibrin-based

bioink was loaded with primary cardiomyocytes isolated from infant rat hearts and was printed inside a PCL frame to form a cardiac patch with biological and mechanical properties similar to the native heart [55]. This construct showed proper maturation of cells *in vitro* and a spontaneous synchronous contraction in the cell culture procedure, which mimicked physiological responses to applied cardiac drugs concerning beating frequency and contraction forces [55].

Fibrin, combined with other natural materials, has also been studied for cardiac 3D printing. One of the most recent studies in this area has conducted by Alonzo et al. This group added the fibrin to a photo-polymerizable gelatin-based bioink to fabricate cardiac cell-laden constructs with the human-induced pluripotent stem cell-derived cardiomyocytes (hiPSCMs), cardiomyocyte cell lines, and cardiac fibroblasts (CFs) [56]. They could fabricate highly porous, networked structures in which the integrated printed cells showed excellent viability, proliferation, and expression of the Troponin-I cardiac marker. Also, in their 3D bioprinted cardiac patch, the coupling between CMs and CFs was promoted, which is the primary step for forming normal physiology for the cardiac wall *in vivo* [56]. Generally, fibrin has shown a recurrent role in the bioengineering of the cardiac tissue [53].

2.3.5 Chitosan

Chitosan is a cationic polysaccharide which is extracted from the chitin of mollusks, crustaceans, and insects [48]. It is non-toxic and biodegradable, and has antibacterial properties [57]. Chitosan is soluble in acidic aqueous solutions, and after neutralization, it forms a gel-like precipitate [58]. Due to this alteration, chitosan has been used in many tissue engineering applications, such as injectable in-situ forming myocardial gels [58][59][60]. Chitosan in cardiac tissue engineering has shown impressive results even by using chemical crosslinking without internal and external architectural design. Chi et al. studied a hybrid cardiac patch made of chitosan combined with silk fibroin-hyaluronic acid [61]. They used genipin to crosslink the hydrogel and then used the hydrogel directly on the MI region in a rat model. The presence of chitosan notably improved neovascularization, secretion of paracrine factors (such as VEGF) in the MI regions, and left ventricular (LV) wall thickness in a rat model. In another study, a cardiac patch comprised of decellularized porcine heart matrix and chitosan showed >80% viability of the cultured neonatal rat ventricular myocytes (NRVM), and chitosan had the leading role in the control of the

degradation rate of the patch [62]. Also, chitosan accompanying polypyrrole as a conductive composite for cardiac tissue engineering has been studied with gel-foaming processes [63].

2.3.6 Alginate

Alginate is a linear block copolymer derived from seaweed. It is a water-soluble negatively charged polysaccharide that becomes a gel in the presence of divalent metal ions such as Ca2+ or Zn2+ [22]. Alginate's non-thrombogenic nature [64] and its ability to form a gel with a porous network make it a suitable material for bioprinting a tissue that can function like native myocardium. This porous structure allows the diffusion of nutrients and waste materials, which is vital for the tissue [65].

Alginate infused with a mixture of pro-survival factors (like stromal cell-derived factor 1 (SDF), insulin-like growth factor 1 (IGF-1)) and angiogenic factors (like VEGF), have been studied in literature and exhibited positive effects on vascularization and viability of the cells in a cardiac patch [66]. Functionalizing the alginate-based scaffolds is also promising for the biological properties of this material [67]. 3D printed sodium alginate modified by the sequence of amino acids (RGD) and laden with human cardiac-derived cardiomyocyte progenitor cells (hCMPCs) has shown an excellent viability rate for the hCMPCs *in vitro* and promoted the differentiation of hCMPCs into cardiomyocyte-like cells [68].

Alginate has also been used in combination with both synthetic and natural materials in cardiac tissue engineering. Alginate modified by polyethylene glycol (PEG) and fibrinogen acted as an encapsulation hydrogel for printing induced pluripotent cell-derived cardiomyocytes (iPSC-CMs) and HUVECs[69]. This cardiac tissue construct had a high orientation index imposed by different defined geometries and blood vessel-like shapes generated by HUVECs. After *in vivo* grafting, this patch showed cell differentiation reinforcement into the cardiomyocyte phenotype, improvement of cardiomyocyte alignment, and promotion of vascularization. Alginate has been used in several cardiovascular 3D printed constructs, such as blood vessel grafts and heart valves, in the literature [70][71].

Alginate is an affordable and manageable ink for 3D bioprinting. It can be crosslinked by different methods, which provides more freedom over the process. For example, printing the alginate solution into the ionic bath, spraying crosslinker solution over the printing strands, adding

the crosslinker into the alginate solution before printing, or combining these methods, can provide a broad spectrum of mechanical and architectural properties.

Typically, natural materials provide better bio-functionality and biocompatibility versus synthetic materials. However, due to their weak mechanical properties, poor handling, and relatively low printing resolution, in many studies, these materials are accompanied by synthetic materials [72][73].

2.4 Synthetic Biomaterials

Synthetic biomaterials have tailor-made characteristics that give us a wide range of choices based on our target application. Among synthetic materials, polymers, metals, and alloys have high popularity of use in biomedical engineering [74]. The most common synthetic biomaterials in 3D printing technologies are polymers [22], especially in cardiovascular tissue engineering [75]. They often provide printability, mechanical support, shape maintenance, and chemical cues for the construct.

2.4.1 Poly-ε-caprolactone (PCL)

PCL is a popular material in different biomedical fields such as bone, cartilage, and heart [76]. It is a low-cost polymer with good processibility and high thermal stability, making it suitable for melt processing. As a result, it enables the fabrication of a variety of structures and forms [77]. Its widespread usage in tissue engineering as the tissue scaffold is also due to its biocompatibility and adjustable degradation rate [78]. However, PCL lacks bioactivity and is hydrophobic. Therefore, low cell affinity and a slow tissue regeneration rate are its negative points [79]. To solve this problem, PCL has been used in combination with more bioactive substances to improve its biological efficiency. PCL has been used in cardiac patches as a component of the scaffold's blend to boost mechanical properties and ease the fabrication process in either electrospinning or 3D printing fabrication methods [80][78]. Benjamin Ho et al. fabricated a 3D extruded PCL scaffold, biologically reinforced by carbon nanotubes (CNTs). They used different percentages of CNT in their blend. The result was significant changes in mechanical properties like elastic modulus and hardness, thermal properties such as degradation temperature, and biological properties such as myocyte attachment to the scaffold due to conductivity [78].

In another study, in a hybrid construct made of heart tissue-derived decellularized extracellular matrix (dECM) bioinks, printed PCL strands collaborated as the mechanical enhancer element. The PCL mesh provided the required stiffness needed for stem cell differentiation. Consequently, high-performance cellular functions such as cell survival, maturation, differentiation, and migration were observed *in vitro* and *in vivo* after implanting the 3D printed tissue construct in mice [35].

PCL can also be used as an attendant compartment for other biomaterials that suffer poor printability and processability. For instance, a composite involving PCL was studied by Yang et al. They used PCL to improve the mechanical properties of polyglycerol sebacate (PGS), specifically its mechanical fracture[81]. This combination could be printed as a highly porous scaffold by adding salt (NaCl) as a curing factor for high temperatures and as a porogen to make hierarchal pores. Due to its desirable elasticity, toughness, and biocompatibility, this patch showed improved cardiac function and positively impacted the progression of left ventricular (LV) remodeling after implantation in the rat model [81].

2.4.2 Polylactic-co-glycolic acid (PLGA)

PLGA is a combination of polylactic acid (PLA) and polyglycolic acid (PGA). The ratio of PLA to PGA changes this polymer's biodegradation rate from a few hours to several years [82]. Electrospun PLGA has been used for cardiac patches combining with different natural compartments such as gelatin [83] or laminin derived biomolecules [84]. Besides, PLGA, as a guidance platform, has been used to direct the organization of the cultured cells to mimic healthy cardiac muscle fibers [85][86]. To do so, in one study, micro-patterned PLGA was cast in fluorinated ethylene propylene (FEP) plates as the mold (solvent casting method), and then human placental choriocarcinoma cell lines were seeded on this micro-grooved PLGA film. As a result, inducible arrhythmias were reduced due to this physical alignment and similar anisotropic electrophysiological features to the native cardiac tissue [85]. This study showed that their patch is considerably more refractory to premature stimuli than the random one constructed with non-grooved PLGA film. In another study, PLGA film was used as a bottom layer for the micro-patterned laminin lanes printed by the micro-contact printing method. Neonatal cardiomyocytes cultured on this patch showed rod-shaped formations with highly aligned myofibrils and bipolar intercalated disks [86].

In contrast with these merits, PLGA is not a highly recommended polymer for 3D printing applications due to its thermosensitivity. High temperatures may lead to structural crosslinking and the formation of toxic components, resulting in unpredictable behavior inside the body [20].

Generally, synthetic biomaterials have good strength and durability. However, their low biocompatibility can create complications. The most pressing concern with these materials is toxicity, especially in biodegradable materials, which can be degraded to potentially harmful byproducts in the body [74]. Therefore, natural biomaterials tend to be a more biocompatible choice for tissue engineering.

2.5 Keys for 3D Printing of Cardiac Patches

Considering tissue engineering strategies in fabricating a cardiac tissue structure can help achieve constructs with a higher capability to mimic the natural tissue and better integration with the rest of the heart. Including cells and neo-vascularization enhancer systems into the 3D printing biomaterial (ink) are two of the common key strategies [87][88].

2.5.1 Cells

After MI, the most irreversible injured part of the heart wall can be the myocardium. Since the numbers of cardiomyocytes are constant from a short time after birth [89], losing a large number of them will considerably weaken the heart's function [90]. Besides, the destructed vascular system on the site is not very helpful for further healing and regeneration. Therefore, many cardiac patches aim to populate the infarcted region with healthy cardiovascular cells [91]. In the bioprinting method, cells can be combined with the printing biomaterial and implanted into the required region after printing. These cells can have various types and be isolated from different donors (Table 2-1 and 2-2).

Table 2-1 Cell source in tissue engineering

		Advantage	Disadvantage	Reference
Cell donors	Autologous	• No risk for host immune response • No disease transmission • Cost-effective	• Limited numbers • Prolonged hospitalization • Extra pain for the patient	[92] [93]
	Syngeneic	• Similar immune system in donor & recipient • Low risk of disease transmission	• Limited numbers	[94] [93]
	Allogeneic	• Abundant availability	• Risk of human disease transmission • Costly	[94] [93] [95]
	Xenogeneic	• Unlimited availability	• Risk of animal-to-human disease transmission • High risk of host rejection • Ethical problems	[93] [96] [97]

Table 2-2 Cell types and derivations for tissue engineering applications

Cell type		Advantage	Disadvantage	Reference
Stem cells	CSC (Cardiac stem cells)	• Cardiac specific differentiation	• Few numbers in natural tissue • Low proliferation capacity	[98] [99]
	MSC (Mesenchymal stem cells)	• Feasible isolation from various tissues • High proliferation rate • Multipotent • Extensive research experience • High paracrine signaling • Low immunogenicity • No arrhythmic risk	• Difficult to extract from tissue • Heterogeneous cell population	[100] [101] [102]
	ESC (Endothelial stem cells)	• Vascularization ability • Highly metabolic • Secreting neuregulin and platelet-derived growth factor subunit β (PDGF-β)	• impaired function in a severe inflammatory situation	[103] [104] [105]

	iPSC (Induced pluripotent stem cell)	• Potential for genetic manipulation • High viability rate	• Risk of arrhythmia • Risk of chromosomal mutation	[106] [102]
Stem cell-derived cells	CMs (Cardiomyocytes)	• Vascularization ability • Highly metabolic • Secreting neuregulin and PDGF-β	• Declining performance with passage • Risk of arrhythmia	[102] [103] [104]
	ECs (Endothelial cells)			
Primary cells	CMs (Cardiomyocytes)	• Normal physiological function	• Difficult to culture and maintain after certain numbers of passage	[107] [108]
	ECs (Endothelial cells)			

2.5.2 Vascularization

One of the main challenges in tissue-engineered constructs is preparing the most appropriate microenvironment for cell adhesion, growth, differentiation, and other biological functions. After MI occurs, severe microvascular damage is seen in a significant number of patients [109]. Therefore, after implanting a cardiac patch, the transfer of nutrient and waste materials to and from the transplanted cells would be a significant concern, especially when the implanted construct is thick. This challenge occurs due to the long distance of cells from the vascular system (especially in the implant's internal parts). On the other hand, vascularization in the infarcted area is too slow and insufficient to solve this problem [110].

In the healthy tissue, signaling molecules in the ECM, such as growth factors and cytokines, promote the biological functions perfectly, leading to tissue health and regeneration [111]. In constructing a tissue in the lab to mimic these processes, a transportation system is required to provide the natural microenvironment for proper supply, recruiting of cells, controlled release of ECM components, and delivery of signaling molecules [112].

Ideally, the mentioned transportation system needs to release its cargo in a sustained, controlled manner, simulating what the real healing system does in the body. This controlled release also is beneficial to reduce the amounts of costly signals, such as growth factors, by exposing them only locally within the patch. Otherwise, tiny and possibly even no growth factor will be received by the implant due to the growth factor being cleared by other body pathways before it reaches the destination site [111].

Various strategies are used to provide a therapeutic sustained-release system within an engineered cardiac patch based on the patch fabrication method. In 3D bioprinting methods, bioinks can contain either vascularization enhancer cells (beneficial in the long term) such as HUVECs, or growth factor cargoes (profitable in a shorter time) such as VEGF. In the first case, the construct's loaded cells can gradually proliferate and secrete ECM with valuable signaling components. Also, vascular cells or stem cells can initiate the formation of vascular networks in the implant site and into the immediate neighborhood to gather body fluids for more integrity. In the second case, patches can be functionalized by an operative growth factor delivery system with controlled released behavior that can gradually deliver an optimal amount of nutrients and drugs to the site’s cells, starting right after implantation.

Nanoparticulate drug delivery systems in which commonly polymeric nanoparticles can be loaded with angiogenetic growth factors such as PDGF, VEGF, and basic fibroblast growth factor (bFGF) [113] are one of the engineering solutions for functionalizing the patches. However, drawbacks such as the unknown fate of nanoparticles, accumulation in other organs [114], risk of crossing the blood-brain barrier [115], and their degradation time and destructive side products [116][117] lead to hesitations in applying them beyond research studies.

Another delivery system for biological factors in tissue engineering scaffolds uses materials that can act as reservoirs and release their attracted growth factors/drugs when the patch's scaffold is degrading. EW is one of these materials that, due to having helical protein structures of albumin (Figure 2-1)[118] has many binding sites and can absorb various drugs. Hence, albumin-based cargo carriers have shown excellent function in drug delivery systems [119].

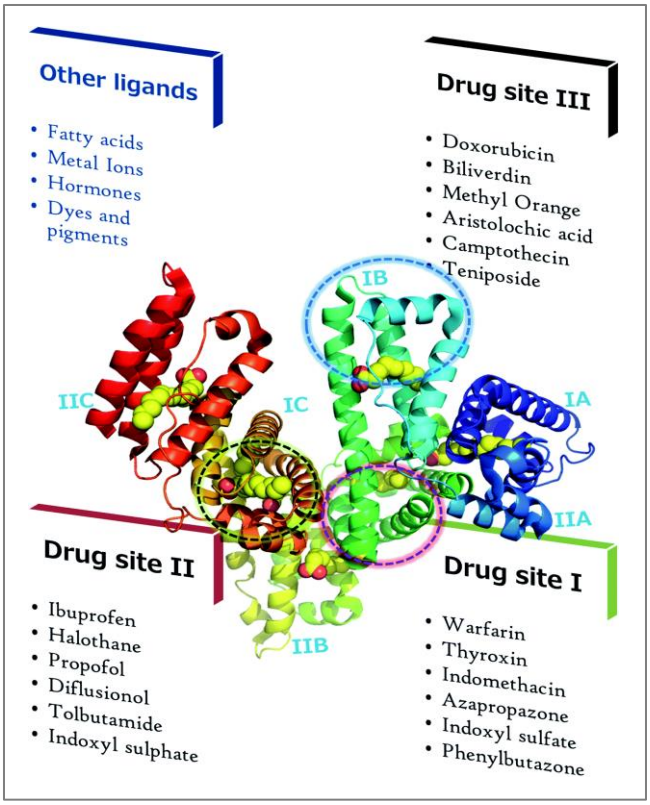

Figure 2-1 Three-dimensional structure of serum albumin and its ligand binding sites

2.6 Physiological Properties and Applications of Egg White in Biomedical Engineering

Among different natural biomaterials, albumin is a highly bioactive, available, and easy to handle material with low production costs compared to other proteins such as collagen or fibronectin [120]. Studies show the albumin biological and mechanical properties as a practical biocompatible biomaterial in tissue engineering and other biomedical research [121][122][123].

Albumin can be derived from a variety of sources. As an autogenic source, a person's blood plasma is enriched with albumin (half of the total protein in the plasma) [122]. However, in a clinical setting, taking the albumin from the patient's blood has a low yield and requires a significant amount of blood, making the procedure invasive [120]. Moreover, appropriate diet and exercise for this harvesting procedure are required, along with accurate monitoring the hemoglobin immunoglobulin, erythrocyte volume, and total serum protein level [124][122].

An off-the-shelf, low-cost alternative source of albumin is egg white (EW). EW's main proteins are ovalbumin, conalbumin, and lysozyme, which have essential biological roles,

including embryo protection and development [125]. Biodegradation of these proteins to their building blocks (amino acids) can provide the required nutrients for cells in their environment [121]. Therefore, chicken EW has been suggested as an available alternative model for 3D cell culture studies [125]. For example, in Guo et al.'s 2017 research, aggregation of ovarian carcinoma cells was observed on the EW constructs fabricated through a cryogelation process. These constructs could provide a suitable mechanical and biological environment for these cells' proliferation and progression [126].

From the biological point of view, albumin as a coating layer in cell culture has shown that it can provide an interface between scaffold and cells and improve the interaction as a mediator. Albumin has shown even better efficiency than collagen and fibronectin in enhancing the cell-material attachment [127]. This material can be degraded by the surrounding cells in the body's environment, and its monomers (amino acids) are biocompatible [127].

Albumin has excellent compatibility with cells and is a good support for the differentiation of stem cells in bone and nerve tissue engineering. Li et al., in 2014, fabricated 3D sponges from enzymatic polymerized albumin as the scaffold for bone tissue regeneration. They cultured human MSCs and showed considerable cell viability and activity even after three days. Furthermore, in the presence of an osteogenic culture medium, seeded MSCs on these sponges showed remarkable osteogenic differentiation [122]. In another study, serum albumin-based fibrous scaffolds showed enhancement of the attachment, proliferation, and neuronal differentiation of hiPSC-derived neural stem cells (NSCs) [128].

Albumin also has suitable mechanical properties such as good elasticity, structural and biochemical properties [122]. Compared to PLLA/ PLGA and PCL nanofibers scaffolds, albumin nanofibrous structures have shown a more similar mechanical behavior to the elastin fibers in connective tissue ECM and had higher flexibility than those scaffolds made of PLLA/ PLGA and PCL [129]. In Nseir, et al.'s 2013 study, albumin-based scaffolds also showed a non-toxic nature and supported adhesion and the spreading of fibroblasts, muscle cells, and endothelial cells (ECs) *in vitro*. The fabricated albumin tubular electrospun structures designed to mimic blood vessels could successfully guide the formation of blood vessel-like bi-layer structures made of fibroblasts and ECs.

Generally, albumin, in addition to supporting cell growth and differentiation, has a desirable protein nature to integrate multiple cues into any tissue-engineered construct and help to

mimic the tissue's natural microenvironment [119]. Accordingly, albumin is also beneficial in cardiac tissue engineering as tissue's scaffold or structural component. In a recent study, Amdursky et al. showed that bovine serum albumin hydrogel has the potential to mimic the rigidity and deformability of the native cardiac tissue [128]. Their albumin-based hydrogel could support the formation of several layers of cardiomyocytes and significantly promoted the maintenance of the gene expression pattern similar to the native heart tissue. As an underlying substrate, this hydrogel showed the ability to induce macroscopic cardiac-like contractions, which could stably function for at least 14 days. The formation of mm-long vascular-like structures resulted from using this albumin-based hydrogel in their study [130]. In another study, electrospun albumin scaffolds showed a similar elastic modulus to the natural cardiac tissue ECM rather than fibers made of PCL that is a commonly used synthetic polymer in fabricating engineered cardiac 3D constructs [121].

Albumin bioengineering applications in the cardiovascular field are not restricted to tissue scaffolds. Sealants are another application for albumin in biomedical research; for example, albumin-based bioGlue acts as a hemostatic adjunct for cardiac and vascular surgeries [131]. Albumin-based sealant has been tested in pigs and has shown excellent expansion and minimal inflammation within three months [132].

Another advantage of albumin that has been substantially emphasized in the literature is its cargo delivery potential because of the albumin protein structure, which has a high affinity to many drugs (Figure 2-1) [118][133][134][119]. This feature makes albumin a decent choice to absorb the cytokines/growth factors from the environment and then release them slowly during the tissue remodeling [63]. In 2015, Jalili et al. fabricated EW albumin sponges for wound-healing applications [120]. Their optimized sponge led to higher angiogenesis than the collagen sponge, which is a commonly used biomaterial in skin repair and tissue engineering [135]. This enhancement was explained as a result of significantly higher adsorption of the proangiogenic vascular endothelial growth factor (VEGF) by their EW scaffolds [120].

Albumin has also been investigated for exhibiting antibacterial behavior. Arzumanyan et al. researched three different types of albumin (bovine serum, human albumin, and ovalbumin) effects on Candida albicans, Cryptococcus neoformans, E. coli, and Staphylococcus aureus cells [136]. All types of their studied albumins showed antimicrobial activity, which leads to a considerable reduction in the number and activity of these microorganisms in the environment.

Also, EW as an embryogenesis environment, has various proteins and enzymes (e.g. lysozyme, which disrupts the bacterial walls) helping to overcome a wide range of microbial microorganisms to protect the embryo [137].

All these properties mentioned for the albumin indicate the biomedical potential of this biological material in diverse areas. EW, as an albumin-enriched, biocompatible, and mechanically strong material, meets the requirements to contribute to tissue patch construction. In the meantime, it can save the expenses of patch sterilization procedures owing to its antibacterial features. Based on these findings, albumin might be a suitable choice as a natural bioink for 3D bioprinting of a cardiac patch.

2.7 Conclusions

This chapter presented a literature review of the biomaterials used in 3D bioprinting and identified the differences and gaps between natural and synthetic materials, which should be noted in creating tissue-like constructs with appropriate mechanical/biological properties. Egg white is a natural, abundant material with a high dose of biological cues and tailorable mechanical properties. This material has shown successful results in cell growth and proliferation in literature along with well-known drug delivery features. Therefore, EW can be a wise choice to be used as a bioink for cardiovascular cells and be 3D bioprinted as an angiogenetic cardiac patch.

Chapter 3: Egg White-Alginate Bioink Development and Patch Bioprinting

3.1 Introduction

For this thesis work, the first step in fabricating the cardiac patch was preparing and characterizing the albumin-based (bio)ink. Due to using an extrusion-based 3D bioplotter, the EW needed to have a certain extrudability. This material also needed to become solid after printing to form a stable 3D printed construct, which could mechanically and biologically be characterized. Sodium alginate, a natural biomaterial with a vast application in 3D bioprinting (discussed in Chapter 2), and possessing an ionic crosslinking procedure, could properly do this job.

In this step of the study, the aim was to gain favorable properties in 3D printing the construct by adding the minimal amount of alginate into the EW to achieve the printability (fine extrusion). Then, rheological characterizations were performed, and suitable blends underwent 3D printing.

3.2 Materials and Methods

3.2.1 Ink Preparation

EW-Alg blends were prepared by adding sodium alginate powder (Medium viscosity, Sigma Aldrich) into pasteurized egg white (purchased from a local grocery store). Five different concentrations of sodium alginate powder in EW were prepared by dissolving 1.0, 1.5, 2.0, 2.5, and 3.0% (w/v) alginate powder in EW fluid and stirring by a magnetic stirrer. After reaching homogeneity, solutions were neutralized to pH∽7 by 0.5 M hydrochloric acid (HCl, 36.5-38.0%, Sigma Aldrich). Later, they were centrifuged to reduce the bubbles formed due to mixing, to obtain a uniform ink (Figure 3-1).

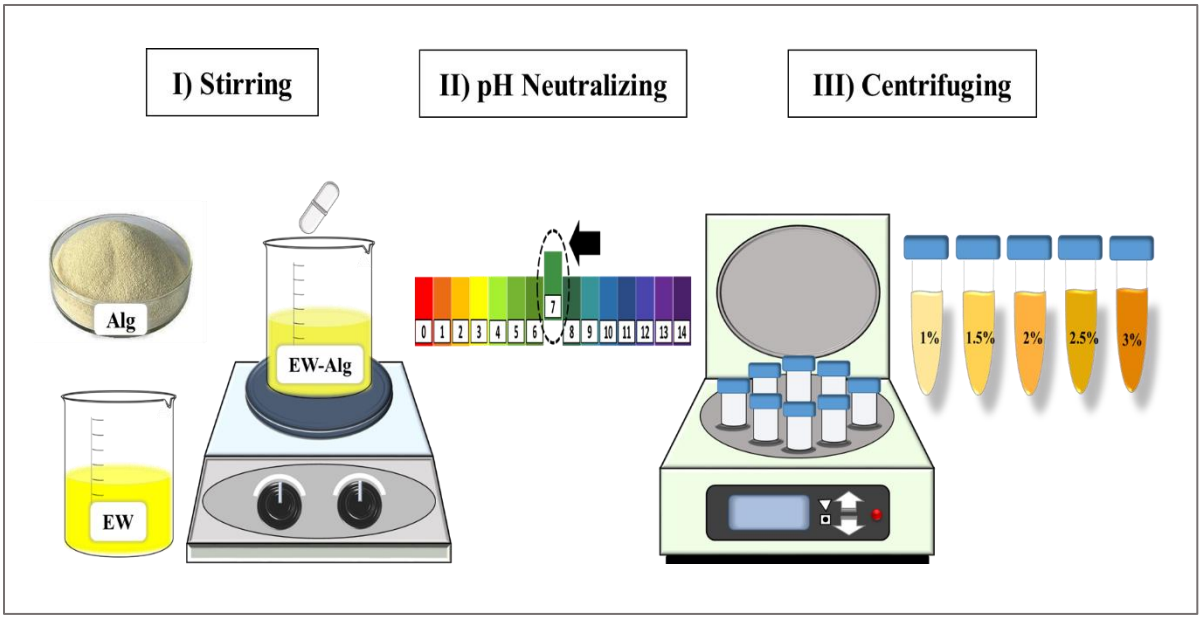

Figure 3-1 Preparation procedure of EW-Alg blends for rheological characterizations and 3D bioprinting

3.2.2 Rheological Characterizations

The flow behavior and viscoelastic properties of the prepared EW-Alg blend were studied using a rheological test on each concentration of the EW-Alg blend at two different temperatures, i.e. 25 °C (room temperature) and 37 °C (body temperature).

Rheological measurements were performed using a rheometer (RVDV-III Ultra Brookfield, USA) with a cone and plate geometry of 40 mm diameter and 2° angle. For every single test, 2 ml of the considered ink was put inside the instrument's plate and heated up to the desired temperature (25 or 37 °C). After reaching the steady-state temperature, rotation started with the speed increments of 5.00, 1.00, 0.50, and 0.10 rpm for the blends of EW-1.5%Alg, EW-2.0%Alg, EW-2.5%Alg, and EW-3.0%Alg, respectively. Shear rate, shear stress, viscosity, and torque were sampled using Brookfield software. Shear stress versus shear rate, and torque versus viscosity graphs were then plotted based on the collected data for each ink. For each concentration, at least five tests were run per each temperature point.

3.2.3 3D Printing of Patches

3D patches were fabricated at room temperature by a pneumatically controlled extrusion-based 3D-bioplotter (EnvisionTEC GmbH) (Figure 3-2). The 3D structure of samples was

designed using Magics EnvisionTEC (V13, Materialise), Bioplotter RP (V2.9, EnvisionTEC GmbH), and Visual Machine BP (V2.2; EnvisionTEC GmbH) software. Patches were printed in 10 layers with a surface area of 12 mm ×12 mm and a height of 8 mm. The inner strands structure was designed as a 1.5 mm distance between strands with a 90° hatch pattern. Plastic dispense tips of gauge 25 (EFD Nordson, USA) were used for manufacturing all the groups. EW-Alg solutions were loaded into the 3D bio-plotter dispenser. A speed of 9, 10 and 11 mm/s, and a pressure of 0.3, 0.5 and 0.8 bar was used to print EW-2.0%Alg, EW-2.5%Alg and EW-3.0%Alg constructs, respectively. Strands were dispensed into 6-well plates containing a crosslinker bath of 25mM $CaCl_2$ and 0.25% (w/v) polyethyleneimine PEI. Printing plates had been coated with 0.1% (w/v) PEI one day before. Patches were kept overnight in 500 mM $CaCl_2$. Then samples were washed five times with distilled water, followed by 70% ethanol, and were then held in PBS overnight to be balanced with a biofidelic fluid before conducting the mechanical characterizations (Figure 3-2).

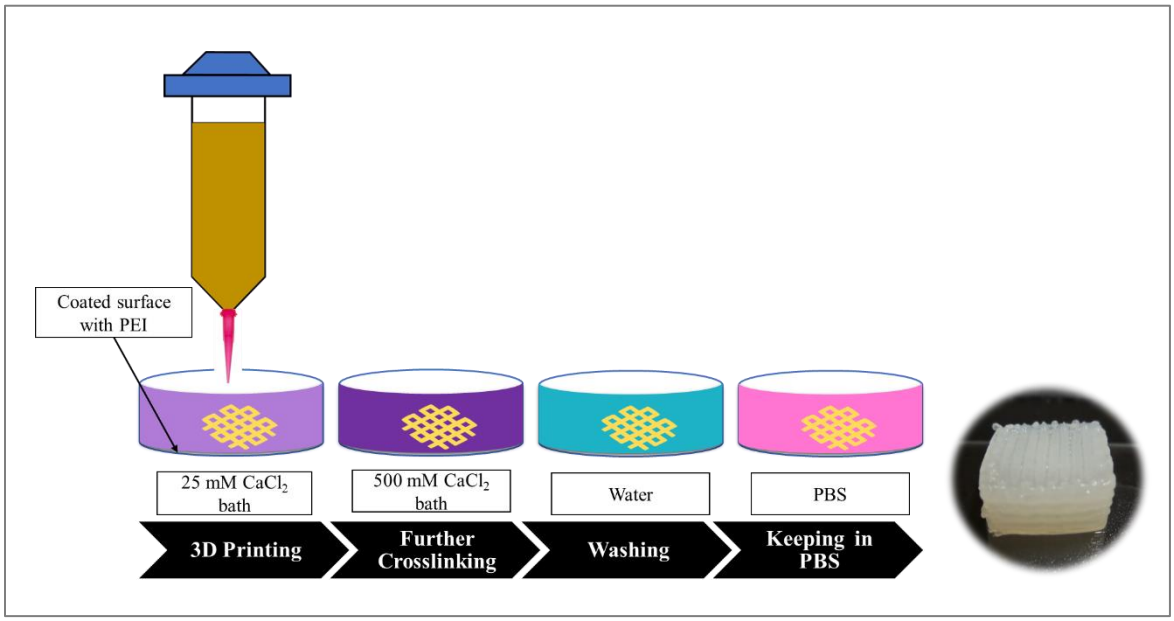

Figure 3-2 The procedure of 3D printing using EW-Alg inks for preparing 10 layer patches

3.3 Results and Discussions

3.3.1 Rheological Studies

Equation 3-1 shows viscosity as a function of shear stress and shear rate for each data point where the τ (Pa) is shear stress, γ (s^{-1}) is the shear rate, and μ demonstrates the viscosity (Pa•s).

$$\mu = \tau/\gamma \qquad (3\text{-}1)$$

Shear stress vs. shear rate and viscosity vs. torque graphs of all samples have been summarized in Figures 3-3 and 3-4. These results showed notable differences among the groups of concentrations. In short, the ink gained a thicker texture and higher viscosity, per 0.5% added alginate. A thicker fluid required more torque to shear off per constant amount of shear rate, and the higher torque indicated a higher amount of shear stress applied.

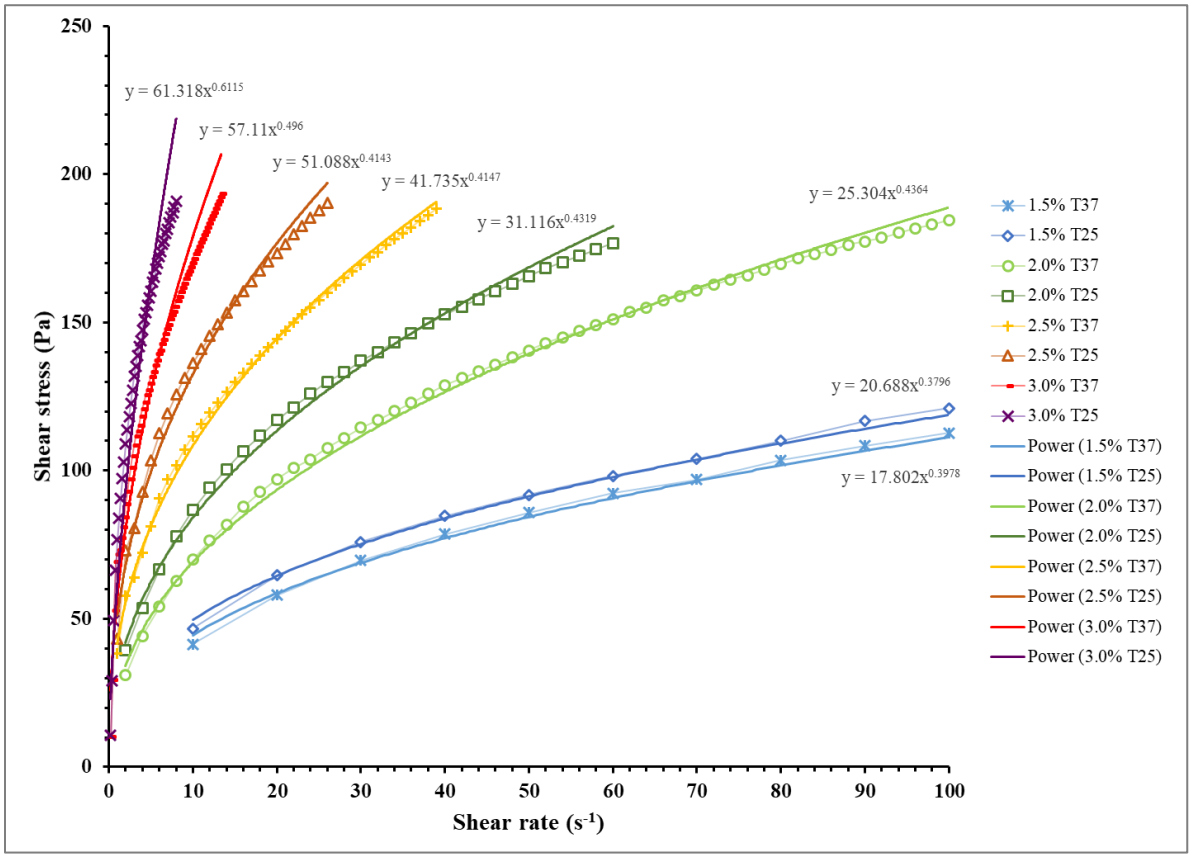

Figure 3-3 Rheological curves of shear stress versus shear rate per percentage of Alg in EW for all prepared EW-Alg blends, in temperatures of 25 ˚C and 37 ˚C. Equations of trendlines are labeled on each curve by Microsoft Excel

In addition to the Alg concentration in the blend, temperature also influenced the EW-Alg fluid thickness. All inks at 25 ˚C possessed a thicker texture compared to their 37 ˚C states; this showed an inverse correlation between the viscosity and temperature. However, the impact of temperature change (from 25 ˚C to 37 ˚C) was not as significant as alginate concentration increments in the inks.

All the blends of EW-Alg showed a non-Newtonian shear-thinning behavior in which when the viscosity decreased the shear strain and torque increased. The best-matched curve following the trend of shear stress vs. shear rate curves for all samples was the power function, as labeled on each curve.

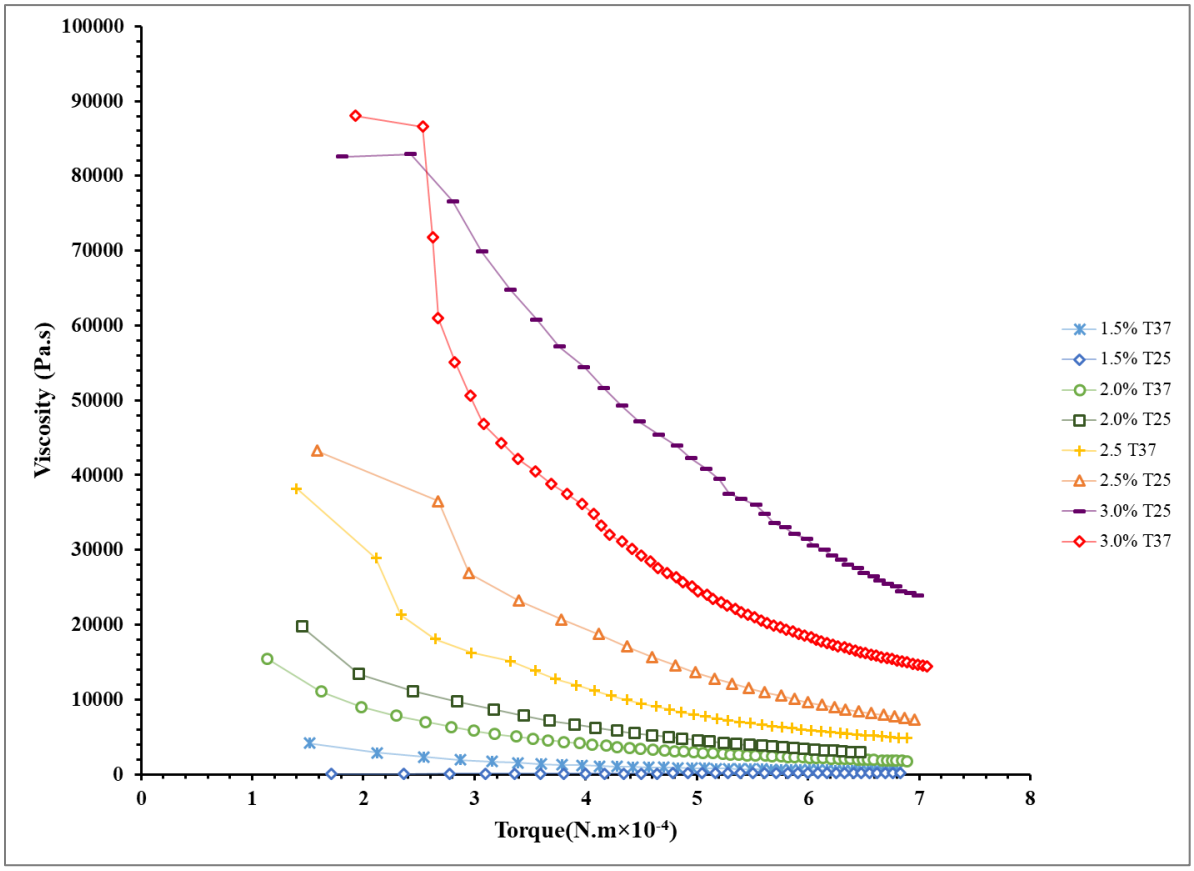

Figure 3-4 Rheological curves of viscosity versus torque for all prepared EW-Alg blends per percentage of Alg in EW, in temperatures of 25 ˚C and 37 ˚C

It is worth pointing out that the blend of EW-1.0%Alg was not thick enough to apply an adequate torque in the measurable range of the rheometer machine to perform the test (% torque <10 for the RVDV-III Ultra Brookfield rheometer, spring torque = 0.7187 mN.m), and an under-range error occurred.

Also, since the shear rate measurements for the EW-1.5%Alg ink exceeded 100 s^{-1}, the shear rate axis was cut in Figure 3-3 for values more than 100 s^{-1} to illustrate all the charts in one graph. Full-range charts are presented in Appendix I.

According to the rheological studies, higher pressures are needed for the extrusion of thicker blends. The higher printing pressure means that biological cells loaded into the bioink may bear higher shear stress levels. Depending on the cell type, high shear stress can be harmful in different ways, such as hurting the cell membrane and/or changing the cell behavior and fate in the long term [138].

3.3.2 Bioprinting Patches

Prepared EW-Alg blends were all tested for their 3D printability. The observed result was that 3D printing was successful on the EW-2.0%Alg, EW-2.5%Alg, and EW-3.0%Alg inks. In these constructs, the shape of 3D printed strands and the hatch angle (90˚) remained accurate after crosslinking and maintained good uniformity (Figure 3-5). For the 3D printing process, as expected from the rheological studies and among the three successful concentrations, EW-2.0%Alg was the ink that used higher speeds and lower pressures to fabricate the same architectural design as in EW-3.0%Alg.

In comparison, the EW-1.0%Alg, and EW-1.5%Alg blends did not exhibit fidelious printability. This lack of feasibility was due to the ink being too watery, lacking extrudability, having too low viscosity, and being unstable during crosslinking. These led to fabrication challenges, such as unattached printed layers, irregular strands, and ink sticking to the dispenser tip (Figure 3-6).

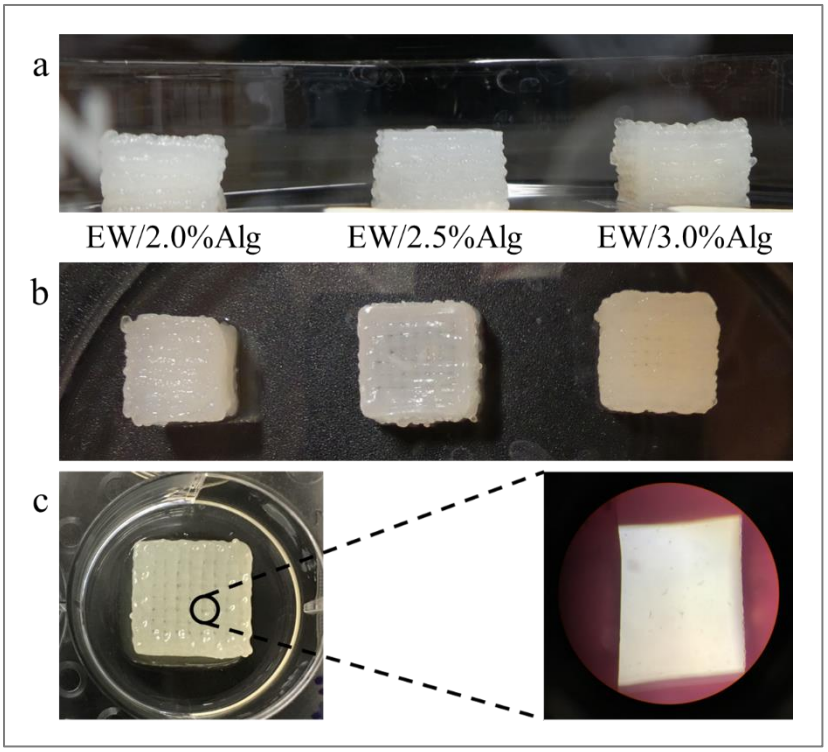

Figure 3-5 3D printed EW-Alg patches from Side view (a), Top view (b), and c) a microscopic view of strands interval with uniform strands

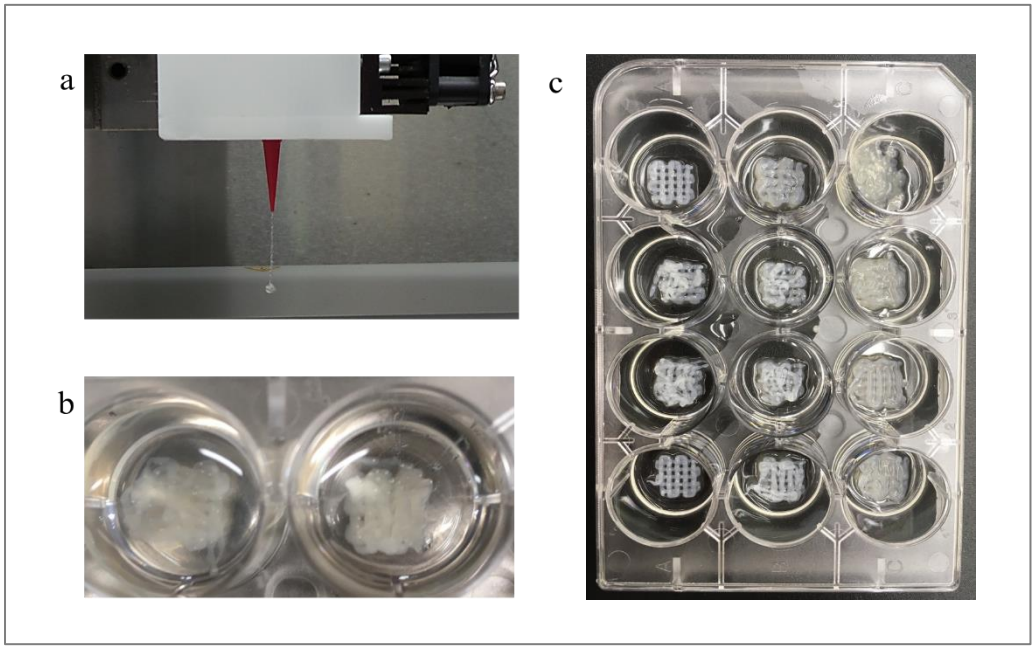

Figure 3-6 Difficulties during the 3D printing procedure of EW-1.5%Alg blend. Unattached strands leading to clogging the needle (a), instability of the printed structure in the crosslinker bath (b), and low fidelity and resolution in printing multi-layer construct

3.4 Conclusions

In fabricating a tissue construct by 3D bioprinting methods, characterization of flow behavior and rheological properties of the printing biomaterial can provide helpful information for predicting the material's parameters during 3D (bio)printing.

In this chapter, EW-Alg blends (inks) were prepared in different ratios of added Alg concentrations. Rheological studies that illustrated the viscosity behavior were performed in two constant temperatures (25 ˚C & 37 ˚C) based on the Alg concentration within the ink. These studies showed a non-Newtonian shear-thinning behavior for all inks, in both temperatures as well as higher shear stresses when running the thicker inks.

The 3D printing procedure was successful only on three concentrations: EW-2.0%Alg, EW-2.5%Alg, and EW-3.0%Alg blends. As the lowest viscosity needed the lowest shear stress during extrusion, EW-1.5%Alg could have been the best choice among the rheologically characterized inks. However, it did not show good fidelity as a hydrogel construct while and after 3D printing. Therefore, the EW-2.0%Alg blend, as the least viscose ink among remaining inks that also presented excellent handling properties with high fidelity in printing, seems to be the best ink to be considered a potential bioink for cells.

Chapter 4: Mechanical Characterization of Egg White-Alginate 3D Printed Patches

4.1 Introduction

After 3D printing the EW-based patches, the mechanical properties of these constructs were investigated to determine (1) if these patches are mechanically reliable to act as successful tissue scaffolds and (2) if changing the concentration of alginate with the step of 0.5% is significantly impacting the mechanical properties of the 3D printed constructs. Thus, the elastic modulus, swelling, and biodegradability of the 3D printed patches were studied and presented in this chapter.

4.2 Materials and Methods

4.2.1 Mechanical Strength Characterization

One of the principle tests to study objects' mechanical strength is conducting a compression test to predict the object's response under compressive loading and its ability to tolerate the applied load without failure or plastic deformation. Herein, this test was performed for investigating the elastic moduli of the 3D printed patches. To do so, unconfined compression at room temperature at a rate of 0.01 mm/s, with a preload of 1 N, was applied on each patch using a biodynamic mechanical testing machine (BioDynamic 5100 Bose). Compressive elastic modulus (E_C), which is the ratio of the applied stress difference to the corresponding strain difference was calculated using the Equations 4-1, 4-2, and 4-3.

$$\sigma = F/A \quad (4\text{-}1)$$

$$\varepsilon = \Delta L/L_0;\ \Delta L = L\text{-}L_0 \quad (4\text{-}2)$$

$$E = \sigma/\varepsilon \quad (4\text{-}3)$$

Where σ is the compressive stress, F - the force, A - the cross-sectional area, ΔL - the change in length, L_0 - the original length, and E is the compression modulus.

More than four samples of each group were tested; and the average values of tests were used to plot the stress versus strain curves.

4.2.2 Swelling and Degradation Characterizations

As myocardial infarction healing is a kind of wound-healing procedure, providing an environment with the ability to absorb water and water-soluble biological cues can keep the wound moisturized and promote faster healing [139]. In this study, the ability of constructs to absorb fluid from the aqueous environment was characterized by a swelling test. In this test, each patch's freeze-dried weight (W_0) was measured. Then, patches were fully immersed in phosphate-buffered saline (PBS) at a 37 °C and 5% CO_2 incubator. After 24 h, swollen patches were taken out of the solution. A filter paper removed the excess solution. Then each wet sample was weighed and this weight was recorded as the wet weight (W_w). The swelling ratio of each sample was calculated according to Equation 4-4:

$$S = [(W_w - W_0)/ W_0] \times 100\% \quad (4\text{-}4)$$

On the other hand, to analyze the 3D printed patches' biodegradation behavior in a body-like environment, lyophilized 3D printed patches were put inside the PBS for 28 days. PBS was changed twice a week to keep the solution fresh with constant ion concentration.

4.2.3 Statistical Analysis

The statistical significance of the results was calculated using a one-way analysis of variance (ANOVA). Pairwise comparisons were performed using the T-test found in Excel. P-values <0.05 were considered statistically significant.

4.3 Results and Discussion

4.3.1 Mechanical Strength

The elastic modulus of each stress/strain curve was obtained by calculating the slope of the linear region of the curve. Figure 4-1 illustrates the results. By increasing the alginate concentration, the elastic modulus increased. This reflected the higher number of crosslinked

structures within the construct due to having a more ionically condensed blend in higher concentrations. i.e. due to having more alginate in the constructs, the ratio of Na^{+} exchanged with Ca^{2+} became greater, and more crosslinking formed stiffer constructs. ANOVA analysis showed a p-value of <0.05 between all groups. Pairwise T-test comparisons showed a significant difference in elastic moduli between EW-2.0%Alg and EW-3.0%Alg samples. In contrast, the alteration is not very notable per each 0.5 % addition of alginate.

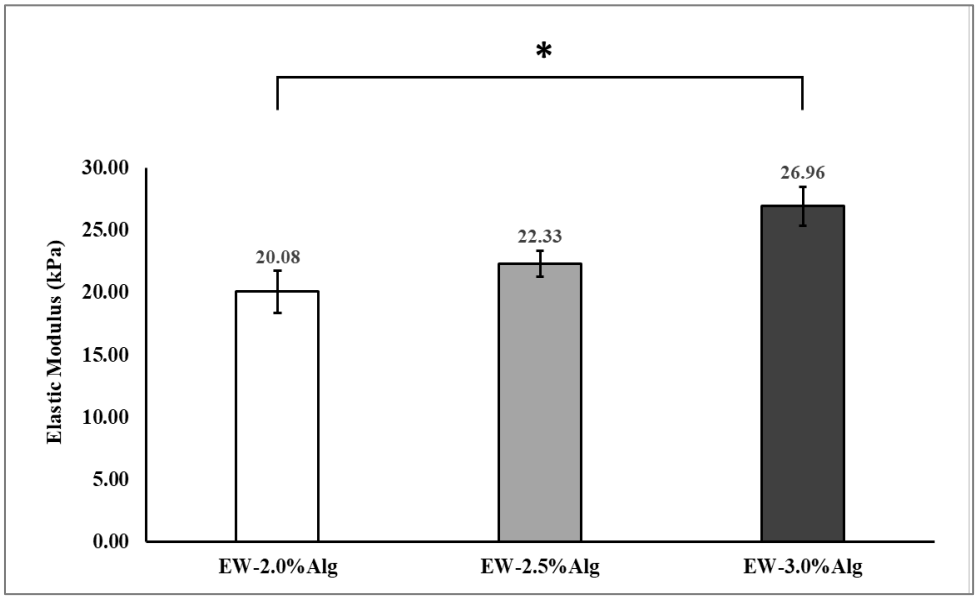

Figure 4-1 Compressive elastic moduli of 3D printed EW-Alg patches ($p<0.05$)

Based on the literature, the human cadaver limb compressive elastic modulus is in the range of ∽20-38 kPa for males and ∽10-32 kPa for females [140]. Furthermore, the porcine cadaver heart (LV part) has shown compressive elastic moduli in the range of ∽2-8.5 kPa and a range of ∽1.5-6 kPa for its decellularized form (heart ECM) [141].

On the other hand, many commercial silicon-based materials used in soft tissue modeling have compressive elastic modulus values close to those of the fabricated EW-Alg patches. Dragon Skin (Smooth-On, Easton, PA) with 20-850 kPa and Semicosil 921 (Wacker Solutions, Adrian, MI) with 25 kPa (Appendix II) [142] are some of these products.

Therefore, as the EW-Alg patches have similar compressive elastic moduli to the mentioned cases, they may have a promising potential to act as a platform in mimicking the soft tissues such as muscles.

4.3.2 Swelling and Degradation Behaviors

All three groups of patches showed swelling ratios of more than 1800%, representing excellent water uptake ability. EW-2.0%Alg patches exhibited the highest values (Figure 4-2). This water storage is a positive feature in tissue engineering since water-soluble growth factors, minerals, and other biological cues can be entrapped within the 3D patch pores and exposed to the implanted cells. The conducted swelling test also indicated that even if these EW-Alg 3D printed constructs are simply used as spongy scaffolds, they can uptake large amounts of body fluid and ions and transform the dry sponge into the wet hydrogel again.

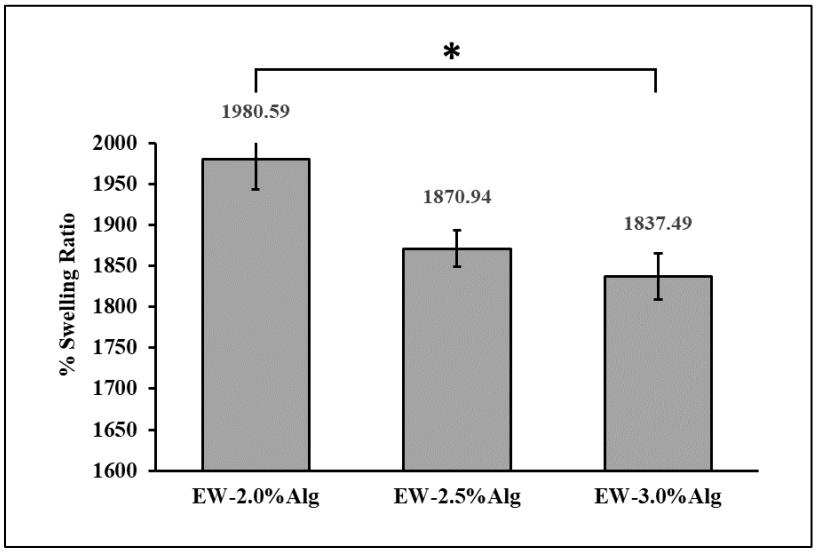

Figure 4-2 Swelling behavior of 3D printed EW-Alg patches after 24h remaining in PBS solution ($p<0.05$)

In the biodegradation test, no weight changes were observed in the samples on days 7, 14, and 21. However, structural destruction of patches was observable and samples were softer in texture. These changes were more tangible after day 21. On day 28, surface strands were being dissociated, and constructs were fragile to touch (Figure 4-3). The day 28 time-point was chosen for observation as it is an average time for the ending stage of cell proliferation, overlapping with the beginning of tissue remodeling. This time is reported as 10-14 days for cutaneous wound healing, 14-35 days for bone remodeling [143], and 14-28 days for ligament repair [144].

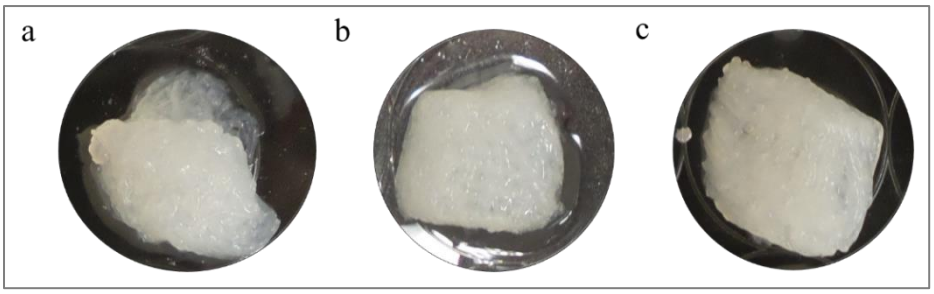

Figure 4-3 Degraded patches made of the blends (a) EW-2.0%Alg, (b) EW-2.5%Alg, and (c) EW-3.0%Alg after 28 days remaining in PBS

In this test, measuring the degradation rate by weight seemed to need a harsher environment like a collagenase enzyme to have measurable weight changes. However, PBS is a frequently used buffer in biological studies, mimicking the human body's osmolality and ion concentrations [145]. It should be pointed out that the 3D patches tested in this chapter were all cell-free constructs. Presenting cells can accelerate the degradation rate as the cells will digest the patch during their proliferation. The other factor is the lack of fluid flow (such as blood flow). The performed degradation test was conducted statically. However, it is expected to have a faster degrading procedure in the presence of body fluids' circulation [146]. In addition, tissue movements (such as heartbeat) might also speed up this degradation rate.

4.4 Conclusions

3D printed patches from the three optimized blends of EW-Alg solutions (2.0, 2.5, and 3.0% alginate in EW) were tested mechanically to determine the best blend to act as a potential bioink (cell-laden ink) in biological studies presented in the next chapter. For this purpose, the elastic modulus, swelling, and degradation behavior of all three groups of 3D printed EW-Alg blends were characterized. As the results showed, all three 3D printed constructs of EW-2.0%Alg, EW-2.5%Alg, and EW-3.0%Alg had mechanical strength similar to cadaver muscle tissues and silicon-based materials used in soft tissue modeling. Particularly, the EW-2.0%Alg patch had the closest elastic modulus to the porcine heart's modulus and its decellularized ECM, measured in literature.

Swelling measurements demonstrated these 3D printed EW-Alg patches' ability to uptake ionic fluids with a slightly higher amount of swelling for the EW-2.0%Alg patch. All of the constructs showed signs of biodegradation within a month, indicating the durability of this patch.

Based on this chapter's results, EW-2.0%Alg ink is considered the optimum solution for being used as a cell-laden bioink.

Chapter 5: *In Vitro* Biological Characterization of the 3D Printed Cardiac Patches

5.1 Introduction

Based on the preceding chapters' results and findings, the EW-2.0%Alg blend was selected as the most suitable (optimum) candidate for cell loading, particularly with the following considerations.

1) It contains the highest amount of egg white (albumin protein) as the leading material with desirable biological cues
2) It has the lowest viscosity, requiring less extruding pressure and shear stress to be applied during the 3D bioprinting procedure.
3) It has the closest elastic modulus to the porcine heart tissue.
4) It shows a strong ability to uptake aqueous fluid and then biodegrades in a biological environment.

In this chapter, EW-2.0%Alg was loaded with HUVECs, which was then bioprinted into cardiac patches. These cell-laden patches were characterized in terms of biocompatibility to see if the performed procedures of patch fabrication (including the biomaterial blending and 3D bioprinting) influenced the cell viability and proliferation within the patches. HUVECs, a type of vascular stem cell, are commonly used in cardiac tissue engineering [147][69]. Therefore, the survival and proliferation of HUVECs can be interpreted as a positive sign of this potential cardiac patch *in vitro.*

5.1.1 Biocompatibility

There are various definitions for the biocompatibility criteria of a material. However, the common point in these definitions is that a biocompatible material can perform its specific application with an appropriate host response [148]. The minimum requirement in this regard is to be non-toxic and/or not to develop toxicity. Biocompatibility can be a grayscale criterion and depends on the application. Enhancing cell proliferation and tissue regeneration can be considered a positive host response in some applications like tissue engineering and a negative reaction in

cancer therapy. Biocompatibility also depends on the duration that the material is supposed to be used [149]. One material can be biocompatible for a specific tissue for a short time but harmful in the same tissue for long-term applications.

5.1.2 *In Vitro* Cell Study

Lab engineered cardiac tissues need to provide conditions that can simulate the natural heart tissue ECM. In this respect, a protein/polysaccharide-based 3D porous environment accompanied by vascular cells might help mimic the initial stages of forming a vascularized cardiac tissue. Therefore, the fabricated EW-Alg patch, having a high amount of amino acids and bioactive sites, was expected to show prosperous cell viability *in vitro*.

5.2 Materials and Methods

5.2.1 Cell Culture

HUVECs (ATCC, Rockville, MD, USA) were cultured in a complete culture medium consisting of Dulbecco's Modified Eagle Medium (L-glucose DMEM, Gibco), 10% hypoxanthine-aminopterin-thymidine (HAT, Gibco), 10% fetal bovine serum (FBS, Gibco), and 1% penicillin-streptomycin antibiotics (PS, Sigma-Aldrich, Canada) [150]. After the cells covered the culture flask (80% confluency), cell passage/subculture was performed. Cells were detached using 0.025% trypsin for 2 minutes in the incubator at 37 °C with 5% CO_2. Trypsin then was neutralized by the complete culture medium (containing FBS). The dissociated cell suspension was centrifuged at 1200 rpm at 4 °C for 5 minutes. The supernatant was removed and the pellet was cultured again. Passage IV cells (with normal activity and confluency) were used for 3D bioprinting.

5.2.2 Cell-Laden Bioink Preparation and 3D Bioprinting

To prepare a bioink, pasteurized EW was mixed with sterilized Alg powder, which formerly was sterilized under a UV lamp (250 nm wavelength) for 2 hours. EW-2.0%Alg blend was prepared and neutralized by filtered HCL to pH∽7. The cultured HUVECs suspension was added to the blend and was gently stirred to achieve a homogenous bioink. All the printing plates (6-well plates) were coated with autoclaved 0.1% (w/v) PEI one day before printing. The cell-

laden bioink was then loaded into the bioplotter dispenser and was 3D bioprinted in the autoclaved $CaCl_2$ bath of 25 mM plus 0.25% PEI. Shortly after printing, the bath was changed with 500 mM $CaCl_2$ for 10 minutes and then was changed with the complete culture medium three times. For this biological assay, 3D patches were bioprinted in 3 layers.

5.2.3 Cell viability assessment

A live/dead assay was performed to observe the cell viability and proliferation of the bioprinted HUVECs within the bioink at different times. This assay is a two-colored staining using fluorescence microscopy. Calcein-AM dye was used for green fluorescent staining of the live cells, indicating the intracellular esterase activity. Simultaneously, Propidium Iodide (PI) was used to red fluorescent stain the dead cells addressing disintegration in their plasma membrane.

Calcein-AM and PI dyes were dissolved in PBS with the final concentration of 1 and 0.5 µL/mL for staining live and dead cells, respectively. For each time point, culture medium was removed from the plates and the dye mixture was added into the 3D bioprinted patches and kept for 30 minutes in the incubator (37 °C, 5% CO_2). Three samples per each time point were imaged using a fluorescence microscope.

The percentage of cell viability was calculated using Equation 5-1, after counting by Image J software.

$$\textit{Cell viability} = (\textit{Live cells}) / (\textit{Live cells} + \textit{Dead cells}) \times 100 \qquad 5\text{-}1$$

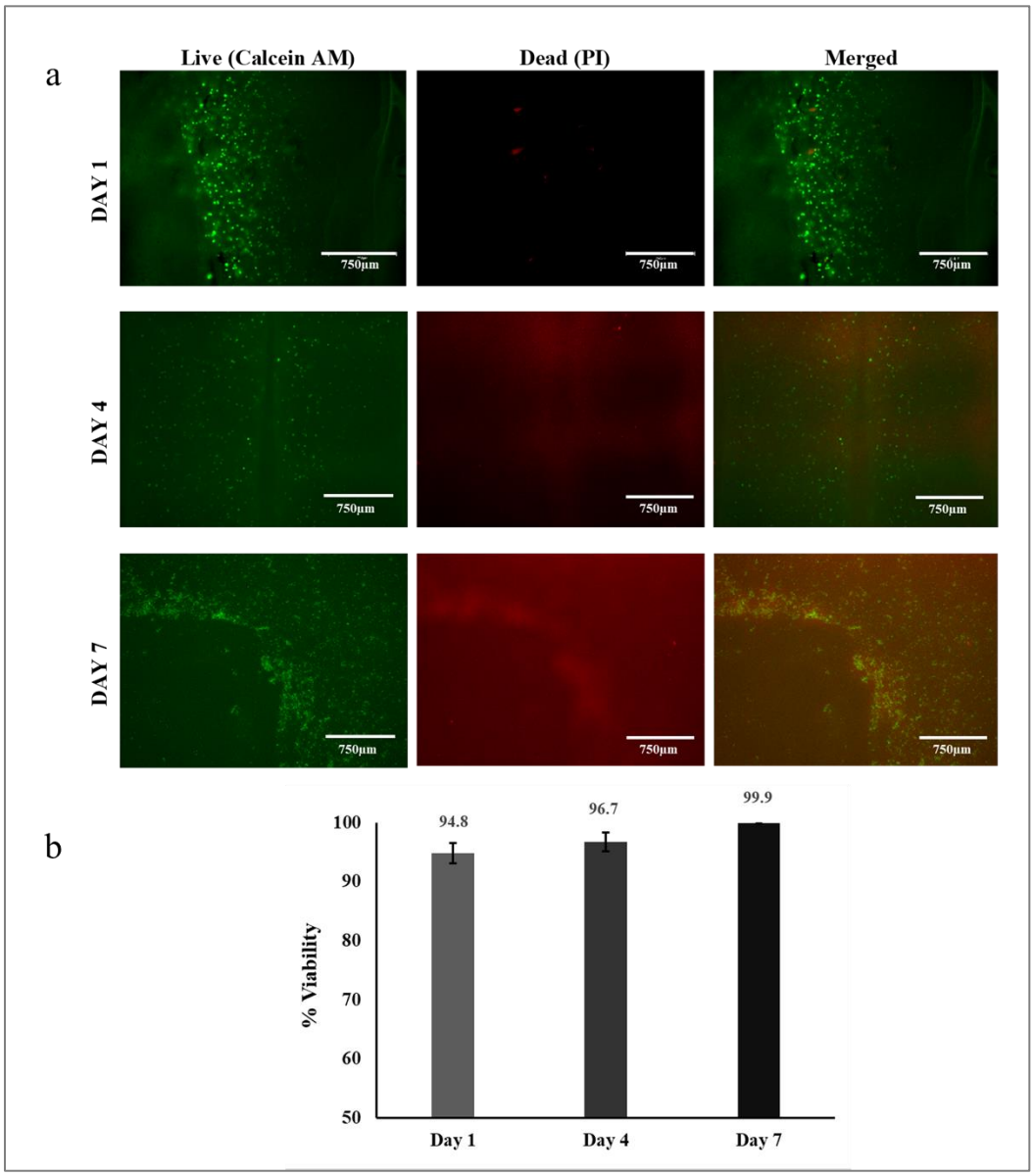

Figure 5-1 Cell viability and proliferation of 3D bioprinted HUVECs within the EW-2.0%Alg bioink by live/dead assay 1, 4, and 7 days after printing. Note (a) fluorescent microscopy, and (b) calculated % cell viability

5.3 Results and Discussion

This patch had the potential to be 3D bioprinted successfully in 12 layers with high fidelity (Figure 5-2).

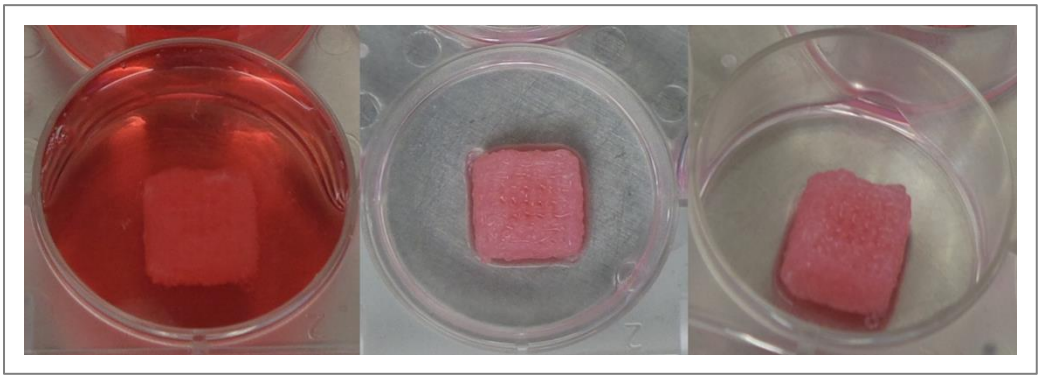

Figure 5-2 3D bioprinted HUVECs-laden potential cardiac patch with 12 layers in complete DMEM from different views

The live/dead assay was conducted on days 1, 4, and 7, after printing. Results in Figure 5-1 show that HUVECs maintained their viability within the 3D printed patch and the ratio of dead to living cells remained very low (<10%) at all the time points after bioprinting. It also showed a high rate of HUVECs proliferation which led to a confluent patch on day 7. The formation of capillary-like structures, visible on day 7 (Figure 5-3) is another affirmative sign for neovascularization and microvessel formation within this cardiac patch.

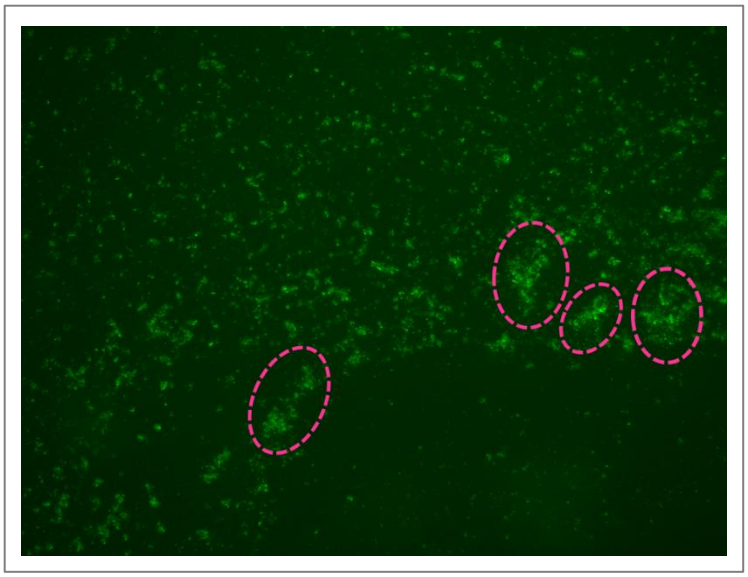

Figure 5-3 Vascular-like HUVECS aggregations (inside dashed areas) within the EW-2.0%Alg bioprinted patch, showing the initial stage of neovascularization

5.4 Conclusions

In this chapter, the optimized EW-Alg blend was utilized as a cell-laden bioink to 3D bioprint the cellular cardiac patches. The 3D bioprinted cardiac patch biocompatibility was tested by investigating the behavior of loaded HUVECs within the 3D construct over seven days. Cell viability was analyzed at 3 time-points: days 1, 4, and 7 post bioprinting. High cell viability (more than 90%) and proliferation were observed. Capillary-like cell aggregations were also evident in the fluorescent microscopy that shows neovascularization initiation within the patches. Therefore, with exhibited positive *in vitro* results, this patch might have good potentials to be characterized *in vivo* for post-MI defects in the future.

Chapter 6: Summary, Conclusions, and Future Prospects

6.1 Summary and Conclusions

In the present study, EW-Alg was developed as a novel bioink for 3D cardiac patch bioprinting; and its potential was investigated in terms of 1) rheologically studying various concentrations of the Alg in EW, and 3D printing the EW-Alg blends, 2) characterizing the mechanical properties of the cell-free 3D patches, and 3) analyzing the biological activity of HUVECs-laden patches made of the best EW-Alg blend.

Four blends of EW-Alg were prepared with varying concentrations of Alg dissolved in EW and then tested in terms of their rheological behavior at two temperatures of 25 and 37 °C, respectively. EW-Alg showed a shear-thinning behavior in which the viscosity was decreasing under increasing shear strain. Raising the Alg concentration in the blend led to higher shear stresses since the fluid became more viscose. Also, temperature showed a reverse correlation with viscosity and the applied shear stress. Based on this experiment, EW-Alg blends with lower amounts of Alg were recommended to use as a bioink, since they would need lower extrusion printing pressure and would experience lower levels of shear stress during the printing procedure.

The EW-Alg blends with varying ratios of EW to Alg were printed to observe if similar 3D constructs were formed visually. The results illustrated that the EW-1.5%Alg blend did not show good fidelity in the 3D printing procedure as it was very watery, while the other three blends successfully formed 3D structures.

The compressive elastic moduli of 3D printed patches were considered a parameter to mimic heart-muscle mechanical properties under physiological compressive forces. Increasing Alg concentrations led to higher elastic moduli since the patches were chemically more crosslinked. All the EW-Alg patches groups showed the elastic moduli (∽20-27 kPa) close to that of the human cadaver limb muscles (∽10-38 kPa) and many commercial silicone biomaterials with soft tissue modeling applications (Appendix II). Among all groups, the EW-2.0%Alg patch had the lowest compression elastic modulus, which was the closest to the measured value for porcine heart and its decellularized ECM in literature (∽1.5-8.5 kPa).

The swelling capacity and degradation behavior of each group of patches were studied in PBS. The 24 h swelling test showed all patches' capacity to absorb ionic fluid was more than 1800%, with a slight difference among groups. This ability shows the spongy potential of EW-Alg patches in absorbing the body fluid from the environment and providing the implanted cells with necessary growth factors and other biological cues.

Degradation of constructs was visible after 28 days in the form of strand disintegration in the meshed 3D EW-Alg patches. This phenomenon shows the biodegradability of the patches, which is a desired feature. One wants this to occur in the body as the tissue is regenerating. Besides, it indicates that the meshed design can still present decent durability until the tissue regenerates. Many natural biomaterials, such as gelatin and collagen, lack this durability and degrade within a short time before the tissue remodeling is completed.

After the performed characterizations, the EW-2.0%Alg was chosen as the optimum bioink for the 3D bioprinting of the cell-laden cardiac patch. A live/dead cell viability assay was performed to show the viability and proliferation of the 3D bioprinted HUVECs. Cell viability of >90% was observed at every time point after bioprinting.

To conclude, in this study, the EW combined with a minimal amount of Alg in the range of 2.0-3.0% (w/v) were synthesized and then successfully printed to form 3D patches; these patches showed mechanical properties similar to the natural ECM, as confirmed by the compressive testing. The EW-2.0%Alg was considered the most appropriate for use as a bioink, and further tested in terms of biocompatibility through HUVECs, illustrating their high cell viability and proliferation within the 3D bioprinted patches.

6.2 Recommendations for future work

Based on the literature and performed work in this thesis, the following recommendations are proposed for further steps:

1- This study has been performed thoroughly in an *in vitro* phase. Considering these results, the cell-laden 3D bioprinted patch has the potential to be implanted in an animal's cardiac infarcted area for *in vivo* studies.

2- In this work, Alg was used to enhance the eggwhite's extrudability for 3D bioprinting. Other natural biomaterials might also be useful in this case. However, various factors should be investigated in each case. For example, crosslinker agents, solvents, and the materials'

processability can be some of these concerns. As part of this thesis work, some pilot studies performed in this regard are presented in Appendix III.

3- The EW-Alg solution in this study was characterized in its intact blend form without any other chemical or biological modification. However, considering the EW as a drug carrier with a high affinity to a wide range of drugs, targeted manipulations might be feasible. For example, combining other biological components into the bioink, such as growth factors or other bioactive molecules, can improve vascularization or direct the stem cells' differentiation.

4- EW-Alg blends can also be heated and form other types of porous structures, which can also be extruded and 3D printed. However, in this case, as they turn into a solid gelly form, incorporating the cells for 3D cell-laden bioprinting becomes almost impossible. The alternative approach would be culturing the cells on a solid 3D printed scaffold. Heating the scaffold in addition to creating a microporous structure within each strand, could also be a decent method of sterilization. Appendix IV shows some effort in this area that was performed as part of this thesis work.

5- In the biological assay portion of this thesis, cell proliferation of the HUVECs was considered the first step in successful tissue regeneration. Albeit, there should be a time that these cells stop/slow down their division after complete tissue formation. This inhibition can be set up by engineering the cell DNA. Moreover, to make a cardiac tissue more similar to the natural one, the type and ratio of somatic cells to stem cells can also impact the regeneration result.

6- As the architectural design, ratio of EW to Alg, preparation, and crosslinking agent can all change the mechanical properties of the 3D printed constructs, the EW-Alg blend might have the potential to be tailored for a wide range of soft and maybe even hard tissue engineering applications.

References

[1] K. Thygesen, J.S. Alpert, H.D. White, Universal definition of myocardial infarction, Circulation. 116 (2007) 2634–2653. doi:10.1161/CIRCULATIONAHA.107.187397.

[2] B. Nadal-Ginard, J. Kajstura, A. Leri, P. Anversa, Myocyte death, growth, and regeneration in cardiac hypertrophy and failure, Circ. Res. 92 (2003) 139–150. doi:10.1161/01.RES.0000053618.86362.DF.

[3] N.R. Smilowitz, A.M. Mahajan, M.T. Roe, A.S. Hellkamp, K. Chiswell, M. Gulati, H.R. Reynolds, Mortality of myocardial infarction by sex, age, and obstructive coronary artery disease status in the ACTION Registry-GWTG (acute coronary treatment and intervention outcomes network Registry-Get with the guidelines), Circ. Cardiovasc. Qual. Outcomes. 10 (2017) 1–8. doi:10.1161/CIRCOUTCOMES.116.003443.

[4] P.A. Iaizzo, Handbook of cardiac anatomy, physiology, and devices, Second, Springer, 2009.

[5] A. Moscona, H. Moscona, The dissociation and aggregation of cells from organ rudiments of the early chick embryo., J. Anat. 86 (1952) 287–301. http://www.ncbi.nlm.nih.gov/pubmed/12980879%0Ahttp://www.pubmedcentral.nih.gov/articlerender.fcgi?artid=PMC1273752.

[6] M.N. Hirt, A. Hansen, T. Eschenhagen, Cardiac tissue engineering : State of the art, Circ. Res. 114 (2014) 354–367. doi:10.1161/CIRCRESAHA.114.300522.

[7] M. Domenech, L. Polo-Corrales, J.E. Ramirez-Vick, D.O. Freytes, Tissue engineering strategies for myocardial regeneration: Acellular versus cellular scaffolds?, Tissue Eng. - Part B Rev. 22 (2016) 438–458. doi:10.1089/ten.teb.2015.0523.

[8] B. Dawn, A.B. Stein, K. Urbanek, M. Rota, B. Whang, R. Rastaldo, D. Torella, X.L. Tang, A. Rezazadeh, J. Kajstura, A. Leri, G. Hunt, J. Varma, S.D. Prabhu, P. Anversa, R. Bolli, Cardiac stem cells delivered intravascularly traverse the vessel barrier, regenerate infarcted myocardium, and improve cardiac function, Proc. Natl. Acad. Sci. U. S. A. 102 (2005) 3766–3771. doi:10.1073/pnas.0405957102.

[9] M.K. Tomasz Siminiak, Pawel Burchardt, Postinfarction heart failure: Surgical and trans-coronary-venous transplantation of autologous myoblasts., Nat. Clin. Pract. Cardiovasc. Med. 3 (2006) 46–51.

[10] D.E. Discher, D.J. Mooney, P.W. Zandstra, Growth factors, matrices, and forces combine, Growth (Lakeland). 324 (2010) 1673–1677. doi:10.1126/science.1171643.Growth.

[11] H. Wang, J. Zhou, Z. Liu, C. Wang, Injectable cardiac tissue engineering for the treatment of myocardial infarction, J. Cell. Mol. Med. 14 (2010) 1044–1055. doi:10.1111/j.1582-4934.2010.01046.x.

[12] T. Kofidis, J.L. De Bruin, G. Hoyt, Y. Ho, M. Tanaka, T. Yamane, D.R. Lebl, R.J. Swijnenburg, C.P. Chang, T. Quertermous, R.C. Robbins, Myocardial restoration with embryonic stem cell bioartificial tissue transplantation, J. Hear. Lung Transplant. 24 (2005) 737–744. doi:10.1016/j.healun.2004.03.023.

[13] R. Parhi, Cross-linked hydrogel for pharmaceutical applications: A review, Adv. Pharm. Bull. 7 (2017) 515–530. doi:10.15171/apb.2017.064.

[14] J. Zhang, Engineered tissue patch for cardiac cell therapy, Curr. Treat. Options Cardiovasc. Med. 17 (2015). doi:10.1007/s11936-015-0399-5.

[15] T. Shimizu, M. Yamato, A. Kikuchi, T. Okano, Cell sheet engineering for myocardial tissue reconstruction, Biomaterials. 24 (2003) 2309–2316. doi:10.1016/S0142-

9612(03)00110-8.
[16] A. Gilpin, Y. Yang, Decellularization strategies for regenerative medicine: From processing techniques to applications, Biomed Res. Int. 2017 (2017). doi:10.1155/2017/9831534.
[17] V.K. Lee, D.Y. Kim, H. Ngo, Y. Lee, L. Seo, S.S. Yoo, P.A. Vincent, G. Dai, Creating perfused functional vascular channels using 3D bio-printing technology, Biomaterials. 35 (2014) 8092–8102. doi:10.1016/j.biomaterials.2014.05.083.
[18] J. An, J.E.M. Teoh, R. Suntornnond, C.K. Chua, Design and 3D printing of scaffolds and tissues, Engineering. 1 (2015) 261–268. doi:10.15302/J-ENG-2015061.
[19] G. Cidonio, M. Glinka, J.I. Dawson, R.O.C. Oreffo, The cell in the ink: Improving biofabrication by printing stem cells for skeletal regenerative medicine, Biomaterials. 209 (2019) 10–24. doi:10.1016/j.biomaterials.2019.04.009.
[20] A. V. Mironov, A.M. Grigoryev, L.I. Krotova, N.N. Skaletsky, V.K. Popov, V.I. Sevastianov, 3D printing of PLGA scaffolds for tissue engineering, J. Biomed. Mater. Res. - Part A. 105 (2017) 104–109. doi:10.1002/jbm.a.35871.
[21] W. Zhu, X. Qu, J. Zhu, X. Ma, S. Patel, J. Liu, P. Wang, C.S.E. Lai, M. Gou, Y. Xu, K. Zhang, S. Chen, Direct 3D bioprinting of prevascularized tissue constructs with complex microarchitecture, Biomaterials. 124 (2017) 106–115. doi:10.1016/j.biomaterials.2017.01.042.
[22] X.B. Chen, Extrusion bioprinting of scaffolds for tissue engineering applications, Springer, 2019. doi:10.1007/978-3-030-03460-3.
[23] M. Qasim, F. Haq, M.H. Kang, J.H. Kim, 3D printing approaches for cardiac tissue engineering and role of immune modulation in tissue regeneration, Int. J. Nanomedicine. 14 (2019) 1311–1333. doi:10.2147/IJN.S189587.
[24] S. Kyle, Z.M. Jessop, A. Al-Sabah, I.S. Whitaker, “Printability” of candidate iomaterials for extrusion based 3D rinting: State-of-the-art, Adv. Healthc. Mater. 6 (2017) 1–16. doi:10.1002/adhm.201700264.
[25] E. Abelardo, Synthetic material bioinks, in: 3D Bioprinting Reconstr. Surg., 2018: pp. 137–144.
[26] Y. Duan, Z. Liu, J. O’Neill, L.Q. Wan, D.O. Freytes, G. Vunjak-Novakovic, Hybrid gel composed of native heart matrix and collagen induces cardiac differentiation of human embryonic stem cells without supplemental growth factors, J. Cardiovasc. Transl. Res. 4 (2011) 605–615. doi:10.1007/s12265-011-9304-0.
[27] J.M. Singelyn, P. Sundaramurthy, T.D. Johnson, P.J. Schup-Magoffin, D.P. Hu, D.M. Faulk, J. Wang, K.M. Mayle, K. Bartels, M. Salvatore, A.M. Kinsey, A.N. Demaria, N. Dib, K.L. Christman, Catheter-deliverable hydrogel derived from decellularized ventricular extracellular matrix increases endogenous cardiomyocytes and preserves cardiac function post-myocardial infarction, J. Am. Coll. Cardiol. 59 (2012) 751–763. doi:10.1016/j.jacc.2011.10.888.
[28] S. Rajabi-Zeleti, S. Jalili-Firoozinezhad, M. Azarnia, F. Khayyatan, S. Vahdat, S. Nikeghbalian, A. Khademhosseini, H. Baharvand, N. Aghdami, The behavior of cardiac progenitor cells on macroporous pericardium-derived scaffolds, Biomaterials. 35 (2014) 970–982. doi:10.1016/j.biomaterials.2013.10.045.
[29] M.Y. Tan, W. Zhi, R.Q. Wei, Y.C. Huang, K.P. Zhou, B. Tan, L. Deng, J.C. Luo, X.Q. Li, H.Q. Xie, Z.M. Yang, Repair of infarcted myocardium using mesenchymal stem cell seeded small intestinal submucosa in rabbits, Biomaterials. 30 (2009) 3234–3240.

doi:10.1016/j.biomaterials.2009.02.013.
[30] P. V. Kochupura, E.U. Azeloglu, D.J. Kelly, S. V. Doronin, S.F. Badylak, I.B. Krukenkamp, I.S. Cohen, G.R. Gaudette, Tissue-engineered myocardial patch derived from extracellular matrix provides regional mechanical function, Circulation. 112 (2005) 144–149. doi:10.1161/CIRCULATIONAHA.104.524355.
[31] A. V. Piterina, A.J. Cloonan, C.L. Meaney, L.M. Davis, A. Callanan, M.T. Walsh, T.M. McGloughlin, ECM-based materials in cardiovascular applications: Inherent healing potential and augmentation of native regenerative processes, Int. J. Mol. Sci. 10 (2009) 4375–4417. doi:10.3390/ijms10104375.
[32] D. Bejleri, M.E. Davis, Decellularized extracellular matrix materials for cardiac repair and regeneration, Adv. Healthc. Mater. 8 (2019) 1–29. doi:10.1002/adhm.201801217.
[33] J. Jang, 3D bioprinting and in vitro cardiovascular tissue modeling, Bioengineering. 4 (2017). doi:10.3390/bioengineering4030071.
[34] D. Bejleri, B.W. Streeter, A.L.Y. Nachlas, M.E. Brown, R. Gaetani, K.L. Christman, M.E. Davis, A bioprinted cardiac patch composed of cardiac-specific extracellular matrix and progenitor cells for heart repair, Adv. Healthc. Mater. 7 (2018) 1–13. doi:10.1002/adhm.201800672.
[35] J. Jang, H.J. Park, S.W. Kim, H. Kim, J.Y. Park, S.J. Na, H.J. Kim, M.N. Park, S.H. Choi, S.H. Park, S.W. Kim, S.M. Kwon, P.J. Kim, D.W. Cho, 3D printed complex tissue construct using stem cell-laden decellularized extracellular matrix bioinks for cardiac repair, Biomaterials. 112 (2017) 264–274. doi:10.1016/j.biomaterials.2016.10.026.
[36] R. Khan, M.H. Khan, Use of collagen as a biomaterial: An update, J. Indian Soc. Periodontol. 17 (2013) 539–542. doi:10.4103/0972-124X.118333.
[37] N.F. Huang, J. Yu, R. Sievers, S. Li, R.J. Lee, Injectable biopolymers enhance angiogenesis after myocardial infarction, Tissue Eng. 11 (2005) 1860–1866. doi:10.1089/ten.2005.11.1860.
[38] J. Li, M. Chen, X. Fan, H. Zhou, Recent advances in bioprinting techniques: Approaches, applications and future prospects, J. Transl. Med. 14 (2016) 1–15. doi:10.1186/s12967-016-1028-0.
[39] J.P. Jung, D.B. Bhuiyan, B.M. Ogle, Solid organ fabrication: Comparison of decellularization to 3D bioprinting, Biomater. Res. 20 (2016) 1–11. doi:10.1186/s40824-016-0074-2.
[40] M. Pauschinger, A. Doerner, A. Remppis, R. Tannhäuser, U. Kühl, H.P. Schultheiss, Differential myocardial abundance of collagen type I and type III mRNA in dilated cardiomyopathy: Effects of myocardial inflammation, Cardiovasc. Res. 37 (1998) 123–129. doi:10.1016/S0008-6363(97)00217-4.
[41] V. Schwach, R. Passier, Native cardiac environment and its impact on engineering cardiac tissue, Biomater. Sci. 7 (2019) 3566–3580. doi:10.1039/c8bm01348a.
[42] A. Tijore, S.A. Irvine, U. Sarig, P. Mhaisalkar, V. Baisane, S. Venkatraman, Contact guidance for cardiac tissue engineering using 3D bioprinted gelatin patterned hydrogel, Biofabrication. 10 (2018). doi:10.1088/1758-5090/aaa15d.
[43] B.J. Klotz, D. Gawlitta, A.J.W.P. Rosenberg, J. Malda, F.P.W. Melchels, Gelatin-methacryloyl hydrogels: towards biofabrication-based tissue repair, Trends Biotechnol. 34 (2016) 394–407. doi:10.1016/j.tibtech.2016.01.002.
[44] P. Koti, N. Muselimyan, E. Mirdamadi, H. Asfour, N.A. Sarvazyan, Use of GelMA for 3D printing of cardiac myocytes and fibroblasts, J. 3D Print. Med. 3 (2019) 11–22.

doi:10.2217/3dp-2018-0017.
[45] R. Gaetani, D.A.M. Feyen, V. Verhage, R. Slaats, E. Messina, K.L. Christman, A. Giacomello, P.A.F.M. Doevendans, J.P.G. Sluijter, Epicardial application of cardiac progenitor cells in a 3D-printed gelatin/hyaluronic acid patch preserves cardiac function after myocardial infarction, Biomaterials. 61 (2015) 339–348. doi:10.1016/j.biomaterials.2015.05.005.
[46] S.M.W. Vahid Serpooshan, Morteza Mahmoudi, Daniel A. Hu, James B. Hu, Bioengineering cardiac constructs using 3D printing., J. 3D Print. Med. 1 (2017).
[47] J. Liu, J. He, J. Liu, X. Ma, Q. Chen, N. Lawrence, W. Zhu, Y. Xu, S. Chen, Rapid 3D bioprinting of in vitro cardiac tissue models using human embryonic stem cell-derived cardiomyocytes, Bioprinting. 13 (2019) 1–6. doi:10.1016/j.bprint.2019.e00040.
[48] M.M.P. and A.V.-L. M. Arnal-Pastor, J. C. Chachques, Biomaterials for Cardiac Tissue Engineering., in: Regen. Med. Tissue Eng., IntechOpen, 2013.
[49] T.P. Martens, A.F.G. Godier, J.J. Parks, L.Q. Wan, M.S. Koeckert, G.M. Eng, B.I. Hudson, W. Sherman, G. Vunjak-Novakovic, Percutaneous cell delivery into the heart using hydrogels polymerizing in situ, Cell Transplant. 18 (2009) 297–304. doi:10.3727/096368909788534915.
[50] O. Gsib, M. Deneufchatel, M. Goczkowski, M. Trouillas, M. Resche-Guigon, S. Bencherif, O. Fichet, J.J. Lataillade, V. Larreta-Garde, C. Egles, FibriDerm: Interpenetrated fibrin scaffolds for the construction of human skin equivalents for full thickness burns, Irbm. 39 (2018) 103–108. doi:10.1016/j.irbm.2017.10.006.
[51] R. Vilar, R.J. Fish, A. Casini, M. Neerman-Arbez, Fibrin(ogen) in human disease: Both friend and foe, Haematologica. 105 (2020) 284–296. doi:10.3324/haematol.2019.236901.
[52] H.-D. Guo, H.-J. Wang, Y.-Z. Tan, and Jin-Hong Wu, Transplantation of marrow-derived cardiac stem cells carried in fibrin improves cardiac function after myocardial infarction, Tissue Eng. Part A. 17 (2010) 45–58.
[53] M.C. Barsotti, F. Felice, A. Balbarini, R. Di Stefano, Fibrin as a scaffold for cardiac tissue engineering, Biotechnol. Appl. Biochem. 58 (2011) 301–310. doi:10.1002/bab.49.
[54] M. Fussenegger, J. Meinhart, W. Höbling, W. Kullich, S. Funk, G. Bernatzky, Stabilized autologous fibrin-chondrocyte constructs for cartilage repair in vivo, Ann. Plast. Surg. 51 (2003) 493–498. doi:10.1097/01.sap.0000067726.32731.E1.
[55] Z. Wang, S.J. Lee, H.J. Cheng, J.J. Yoo, A. Atala, 3D bioprinted functional and contractile cardiac tissue constructs, Acta Biomater. 70 (2018) 48–56. doi:10.1016/j.actbio.2018.02.007.
[56] M. Alonzo, S. AnilKumar, B. Roman, N. Tasnim, B. Joddar, 3D Bioprinting of cardiac tissue and cardiac stem cell therapy, Transl. Res. 211 (2019) 64–83. doi:10.1016/j.trsl.2019.04.004.
[57] Y. Pang, A. Qin, X. Lin, L. Yang, Q. Wang, Z. Wang, Z. Shan, S. Li, J. Wang, S. Fan, Q. Hu, Biodegradable and biocompatible high elastic chitosan scaffold is cell-friendly both in vitro and in vivo , Oncotarget. 8 (2017) 35583–35591. doi:10.18632/oncotarget.14709.
[58] A. Chenite, C. Chaput, D. Wang, C. Combes, M.D. Buschmann, C.D. Hoemann, J.C. Leroux, B.L. Atkinson, F. Binette, A. Selmani, Novel injectable neutral solutions of chitosan form biodegradable gels in situ, Biomaterials. 21 (2000) 2155–2161. doi:10.1016/S0142-9612(00)00116-2.
[59] B. Xu, Y. Li, B. Deng, X. Liu, L. Wang, Q.L. Zhu, Chitosan hydrogel improves mesenchymal stem cell transplant survival and cardiac function following myocardial

infarction in rats, Exp. Ther. Med. 13 (2017) 588–594. doi:10.3892/etm.2017.4026.
[60] B.H. Liu, H.Y. Yeh, Y.C. Lin, M.H. Wang, D.C. Chen, B.H. Lee, S.H. Hsu, Spheroid formation and enhanced cardiomyogenic potential of adipose-derived stem cells grown on chitosan, Biores. Open Access. 2 (2013) 28–39. doi:10.1089/biores.2012.0285.
[61] N.H. Chi, M.C. Yang, T.W. Chung, N.K. Chou, S.S. Wang, Cardiac repair using chitosan-hyaluronan/silk fibroin patches in a rat heart model with myocardial infarction, Carbohydr. Polym. 92 (2013) 591–597. doi:10.1016/j.carbpol.2012.09.012.
[62] S. Pok, O.M. Benavides, P. Hallal, J.G. Jacot, Use of myocardial matrix in a chitosan-based full-thickness heart patch, Tissue Eng. - Part A. 20 (2014) 1877–1887. doi:10.1089/ten.tea.2013.0620.
[63] S. He, H. Song, J. Wu, S.H. Li, R.D. Weisel, H.W. Sung, J. Li, R.K. Li, Preservation of conductive propagation after surgical repair of cardiac defects with a bio-engineered conductive patch, J. Hear. Lung Transplant. 37 (2018) 912–924. doi:10.1016/j.healun.2017.12.011.
[64] J.R. Venugopal, M.P. Prabhakaran, S. Mukherjee, R. Ravichandran, K. Dan, S. Ramakrishna, Biomaterial strategies for alleviation of myocardial infarction, J. R. Soc. Interface. 9 (2012) 1–19. doi:10.1098/rsif.2011.0301.
[65] C.S. Ong, L. Nam, K. Ong, A. Krishnan, C.Y. Huang, T. Fukunishi, N. Hibino, 3D and 4D bioprinting of the myocardium: Current approaches, challenges, and future prospects, Biomed Res. Int. 2018 (2018). doi:10.1155/2018/6497242.
[66] T. Dvir, A. Kedem, E. Ruvinov, O. Levy, I. Freeman, N. Landa, R. Holbova, M.S. Feinberg, S. Dror, Y. Etzion, J. Leor, S. Cohen, Prevascularization of cardiac patch on the omentum improves its therapeutic outcome, Proc. Natl. Acad. Sci. U. S. A. 106 (2009) 14990–14995. doi:10.1073/pnas.0812242106.
[67] K.Y. Lee, D.J. Mooney, Alginate: Properties and biomedical applications, Prog. Polym. Sci. 37 (2012) 106–126. doi:10.1016/j.progpolymsci.2011.06.003.
[68] R. Gaetani, P.A. Doevendans, C.H.G. Metz, J. Alblas, E. Messina, A. Giacomello, J.P.G. Sluijter, Cardiac tissue engineering using tissue printing technology and human cardiac progenitor cells, Biomaterials. 33 (2012) 1782–1790. doi:10.1016/j.biomaterials.2011.11.003.
[69] F. Maiullari, M. Costantini, M. Milan, V. Pace, M. Chirivì, S. Maiullari, A. Rainer, D. Baci, H.E.S. Marei, D. Seliktar, C. Gargioli, C. Bearzi, R. Rizzi, A multi-cellular 3D bioprinting approach for vascularized heart tissue engineering based on HUVECs and iPSC-derived cardiomyocytes, Sci. Rep. 8 (2018) 1–15. doi:10.1038/s41598-018-31848-x.
[70] B. Duan, L.A. Hockaday, K.H. Kang, J.T. Butcher, 3D Bioprinting of heterogeneous aortic valve conduits with alginate/gelatin hydrogels, J. Biomed. Mater. Res. - Part A. 101 A (2013) 1255–1264. doi:10.1002/jbm.a.34420.
[71] G. Gao, J.H. Lee, J. Jang, D.H. Lee, J.S. Kong, B.S. Kim, Y.J. Choi, W.B. Jang, Y.J. Hong, S.M. Kwon, D.W. Cho, Tissue engineered bio-blood-vessels constructed using a tissue-specific bioink and 3D coaxial cell printing technique: A novel therapy for ischemic disease, Adv. Funct. Mater. 27 (2017) 1–12. doi:10.1002/adfm.201700798.
[72] A.S. Hoffman, Hydrogels for biomedical applications, Adv. Drug Deliv. Rev. 64 (2012) 18–23. doi:10.1016/j.addr.2012.09.010.
[73] M.M. Stanton, J. Samitier, S. Sánchez, Bioprinting of 3D hydrogels, Lab Chip. 15 (2015) 3111–3115. doi:10.1039/c5lc90069g.
[74] M.T. Lam, J.C. Wu, Biomaterial applications in cardiovascular tissue repair and

regeneration, Expert Rev. Cardiovasc. Ther. 10 (2012) 1039–1049. doi:10.1586/erc.12.99.
[75] A. Moorthi, Y.C. Tyan, T.W. Chung, Surface-modified polymers for cardiac tissue engineering, Biomater. Sci. 5 (2017) 1976–1987. doi:10.1039/c7bm00309a.
[76] N. Siddiqui, S. Asawa, B. Birru, R. Baadhe, S. Rao, PCL-based composite scaffold matrices for tissue engineering applications, Mol. Biotechnol. 60 (2018) 506–532. doi:10.1007/s12033-018-0084-5.
[77] H.S. Yu, J. Park, H.-S. Lee, S.A. Park, D.-W. Lee, K. Park, Feasibility of polycaprolactone scaffolds fabricated by three-dimensional printing for tissue engineering of tunica albuginea, World J. Mens. Health. 36 (2018) 66. doi:10.5534/wjmh.17025.
[78] C.M.B. Ho, A. Mishra, P.T.P. Lin, S.H. Ng, W.Y. Yeong, Y.J. Kim, Y.J. Yoon, 3D printed polycaprolactone carbon nanotube composite scaffolds for cardiac tissue engineering, Macromol. Biosci. 17 (2017) 1–9. doi:10.1002/mabi.201600250.
[79] T. Patrício, M. Domingos, A. Gloria, P. Bártolo, Characterisation of PCL and PCL/PLA scaffolds for tissue engineering, Procedia CIRP. 5 (2013) 110–114. doi:10.1016/j.procir.2013.01.022.
[80] Y. Chen, D. Zeng, L. Ding, X.L. Li, X.T. Liu, W.J. Li, T. Wei, S. Yan, J.H. Xie, L. Wei, Q.S. Zheng, Three-dimensional poly-(ε-caprolactone) nanofibrous scaffolds directly promote the cardiomyocyte differentiation of murine-induced pluripotent stem cells through Wnt/β-catenin signaling, BMC Cell Biol. 16 (2015) 1–13. doi:10.1186/s12860-015-0067-3.
[81] Y. Yang, D. Lei, S. Huang, Q. Yang, B. Song, Y. Guo, A. Shen, Z. Yuan, S. Li, F.L. Qing, X. Ye, Z. You, Q. Zhao, Elastic 3D-printed hybrid polymeric scaffold improves cardiac remodeling after myocardial infarction, Adv. Healthc. Mater. 8 (2019) 1–15. doi:10.1002/adhm.201900065.
[82] M. Hirenkumar, S. Steven, Poly lactic-co-glycolic acid (PLGA) as biodegradable controlled drug delivery carrier, Polymers (Basel). 3 (2012) 1–19. doi:10.3390/polym3031377.Poly.
[83] M.P. Prabhakaran, D. Kai, L. Ghasemi-Mobarakeh, S. Ramakrishna, Electrospun biocomposite nanofibrous patch for cardiac tissue engineering, Biomed. Mater. 6 (2011). doi:10.1088/1748-6041/6/5/055001.
[84] J. Yu, A.R. Lee, W.H. Lin, C.W. Lin, Y.K. Wu, W.B. Tsai, Electrospun PLGA fibers incorporated with functionalized biomolecules for cardiac tissue engineering, Tissue Eng. - Part A. 20 (2014) 1896–1907. doi:10.1089/ten.tea.2013.0008.
[85] Y. Chen, J. Wang, B. Shen, C.W.Y. Chan, C. Wang, Y. Zhao, H.N. Chan, Q. Tian, Y. Chen, C. Yao, I.M. Hsing, R.A. Li, H. Wu, Engineering a freestanding biomimetic cardiac patch using biodegradable poly(lactic-co-glycolic acid) (PLGA) and human embryonic stem cell-derived ventricular cardiomyocytes (hESC-VCMs), Macromol. Biosci. 15 (2015) 426–436. doi:10.1002/mabi.201400448.
[86] T.C. Mcdevitt, J.C. Angello, M.L. Whitney, H. Reinecke, S.D. Hauschka, C.E. Murry, P.S. Stayton, In vitro generation of differentiated cardiac myofibers on micropatterned laminin surfaces, J. Biomed. Mater. Res. 60 (2002) 472–479. doi:10.1008/jbm.1292.
[87] E.C. Novosel, C. Kleinhans, P.J. Kluger, Vascularization is the key challenge in tissue engineering, Adv. Drug Deliv. Rev. 63 (2011) 300–311. doi:10.1016/j.addr.2011.03.004.
[88] G. Vunjak-Novakovic, N. Tandon, A. Godier, R. Maidhof, A. Marsano, T.P. Martens, M. Radisic, Challenges in cardiac tissue engineering., Tissue Eng. Part B. Rev. 16 (2010) 169–187. doi:10.1089/ten.teb.2009.0352.

[89] K.E. Yutzey, Cardiomyocyte Proliferation: Teaching an old dogma new tricks, Circ. Res. 120 (2017) 627–629. doi:10.1161/circresaha.116.310058.
[90] J.P.M. Cleutjens, W.M. Blankesteijn, M.J.A.P. Daemen, J.F.M. Smits, The infarcted myocardium: Simply dead tissue, or a lively target for therapeutic interventions, Cardiovasc. Res. 44 (1999) 232–241. doi:10.1016/S0008-6363(99)00212-6.
[91] E. Ruvinov, Y. Shandalov, S. Levenberg, S. Cohen, Principles of cardiovascular tissue engineering, in: Tissue Eng. (Second Ed., 2014: pp. 627–683.
[92] M.S. Penn, G.S. Francis, S.G. Ellis, J.B. Young, P.M. McCarthy, E.J. Topol, Autologous cell transplantation for the treatment of damaged myocardium, Prog. Cardiovasc. Dis. 45 (2002) 21–32. doi:10.1053/pcad.2002.123466.
[93] H.S. Lee, S.H. Byun, S.W. Cho, B.E. Yang, Past, present, and future of regeneration therapy in oral and periodontal tissue: A review, Appl. Sci. 9 (2019). doi:10.3390/app9061046.
[94] J.W. Hwang, N.K. Lee, J.H. Yang, H.J. Son, S.I. Bang, J.W. Chang, D.L. Na, A comparison of immune responses exerted following syngeneic, allogeneic, and xenogeneic transplantation of mesenchymal stem cells into the mouse brain, Int. J. Mol. Sci. 21 (2020). doi:10.3390/ijms21093052.
[95] C. Blanche, A. Kamlot, D.A. Blanche, B. Kearney, K.E. Magliato, L.S.C. Czer, A. Trento, Heart transplantation with donors fifty years of age and older, J. Thorac. Cardiovasc. Surg. 123 (2002) 810–815. doi:10.1067/mtc.2002.120009.
[96] G. Turco, D. Porrelli, E. Marsich, F. Vecchies, T. Lombardi, C. Stacchi, R. Di Lenarda, Three-dimensional bone substitutes for oral and maxillofacial surgery: Biological and structural characterization, J. Funct. Biomater. 9 (2018). doi:10.3390/jfb9040062.
[97] S. Yeleswarapu, S. Chameettachal, A. Kumar Bera, F. Pati, Tissue-specific bioink from xenogeneic sources for 3D bioprinting of tissue constructs, in: Xenotransplantation, 2020.
[98] S. Maltais, S.J. Joggerst, A. Hatzopoulos, T.G. Disalvo, D. Zhao, H.-J. Sung, X. Wang, J.G. Byrne, A.J. Naftilan, Stem cell therapy for chronic heart failure: an updated appraisal, Expert Opin. Biol. Ther. 13 (2013) 503–516.
[99] W.E. Wang, X. Chen, S.R. Houser, C. Zeng, Potential of cardiac stem/progenitor cells and induced pluripotent stem cells for cardiac repair in ischaemic heart disease, Clin. Sci. 125 (2013) 319–327. doi:10.1042/CS20130019.
[100] A. Dehghanifard, M. Shahjahani, M. Soleimani, N. Saki, The emerging role of mesenchymal stem cells in tissue engineering, Int. J. Hematol. Stem Cell Res. 7 (2013) 43–44.
[101] A. Matsiko, T.J. Levingstone, F.J. O'Brien, Advanced strategies for articular cartilage defect repair, Materials (Basel). 6 (2013) 637–668. doi:10.3390/ma6020637.
[102] R. Guo, M. Morimatsu, T. Feng, F. Lan, D. Chang, F. Wan, Y. Ling, Stem cell-derived cell sheet transplantation for heart tissue repair in myocardial infarction, Stem Cell Res. Ther. 11 (2020) 1–13. doi:10.1186/s13287-019-1536-y.
[103] P.C.H. Hsieh, M.E. Davis, L.K. Lisowski, R.T. Lee, Endothelial-cardiomyocyte interactions in cardiac development and repair, Annu. Rev. Physiol. 68 (2006) 51–66. doi:10.1146/annurev.physiol.68.040104.124629.
[104] H. Sekine, T. Shimizu, K. Hobo, S. Sekiya, J. Yang, M. Yamato, H. Kurosawa, E. Kobayashi, T. Okano, Endothelial cell coculture within tissue-engineered cardiomyocyte sheets enhances neovascularization and improves cardiac function of ischemic hearts., Circulation. 118 (2008) 145–152. doi:10.1161/CIRCULATIONAHA.107.757286.

[105] C.P. Lin, F.Y. Lin, P.H. Huang, Y.L. Chen, W.C. Chen, H.Y. Chen, Y.C. Huang, W.L. Liao, H.C. Huang, P.L. Liu, Y.H. Chen, Endothelial progenitor cell dysfunction in cardiovascular diseases: Role of reactive oxygen species and inflammation, Biomed Res. Int. 2013 (2013). doi:10.1155/2013/845037.
[106] L. Spohn, C. Fichter, M. Werner, S. Lassmann, Subcellular localization of EGFR in esophageal carcinoma cell lines, J. Cell Commun. Signal. 10 (2016) 41–47. doi:10.1007/s12079-015-0308-4.
[107] J. Welser, The advantages and difficulties of working with primary cells, Sci. Res. Lab. (2016).
[108] B.J. Li, P.H. Li, R.H. Huang, W.X. Sun, H. Wang, Q.F. Li, J. Chen, W.J. Wu, H.L. Liu, Isolation, culture and identification of porcine skeletal muscle satellite cells, Asian-Australasian J. Anim. Sci. 28 (2015) 1171–1177. doi:10.5713/ajas.14.0848.
[109] L. Hueso, C. Rios-Navarro, A. Ruiz-Sauri, F.J. Chorro, J. Nunez, M.J. Sanz, V. Bodi, L. Piqueras, Dynamics and implications of circulating anti-angiogenic VEGF-A165b isoform in patients with ST-elevation myocardial infarction, Sci. Rep. 7 (2017) 1–14. doi:10.1038/s41598-017-10505-9.
[110] A. Perets, Y. Baruch, F. Weisbuch, G. Shoshany, G. Neufeld, S. Cohen, Enhancing the vascularization of three-dimensional porous alginate scaffolds by incorporating controlled release basic fibroblast growth factor microspheres, J. Biomed. Mater. Res. - Part A. 65 (2003) 489–497. doi:10.1002/jbm.a.10542.
[111] D.F.W. Clemens Van Blitterswijk, Jan De Boer, Peter Thomsen, Jeffrey Hubbell, Ranieri Cancedda, J.D. de Bruijn, Anders Lindahl, Jerome Sohier, Controlled release strategies in tissue engineering, in: Tissue Eng., Academic Press, 2008: pp. 455–482.
[112] X.C. and M.E.K. Mohammad Izadifar, Azita Haddadi, Rate-programming of nano-particulate delivery systems for smart bioactive scaffolds in tissue engineering, Nanotechnology. 26 (2015).
[113] M. Izadifar, M.E. Kelly, X. Chen, Regulation of sequential release of growth factors using bilayer polymeric nanoparticles for cardiac tissue engineering, Nanomedicine. 11 (2016) 3237–3259. doi:10.2217/nnm-2016-0220.
[114] W.H. De Jong, P.J.A. Borm, Drug delivery and nanoparticles: Applications and hazards, Int. J. Nanomedicine. 3 (2008) 133–149. doi:10.2147/ijn.s596.
[115] D.M. Teleanu, C. Chircov, A.M. Grumezescu, A. Volceanov, R.I. Teleanu, Blood-brain delivery methods using nanotechnology, Pharmaceutics. 10 (2018) 1–16. doi:10.3390/pharmaceutics10040269.
[116] S. Sharma, A. Parmar, S. Kori, R. Sandhir, PLGA-based nanoparticles: A new paradigm in biomedical applications, TrAC - Trends Anal. Chem. 80 (2016) 30–40. doi:10.1016/j.trac.2015.06.014.
[117] I. Khan, K. Saeed, I. Khan, Nanoparticles: Properties, applications and toxicities, Arab. J. Chem. 12 (2019) 908–931. doi:10.1016/j.arabjc.2017.05.011.
[118] S. Awasthi, N.T. Saraswathi, Non-enzymatic glycation mediated structure-function changes in proteins: Case of serum albumin, RSC Adv. 6 (2016) 90739–90753. doi:10.1039/c6ra08283a.
[119] M.T. Larsen, M. Kuhlmann, M.L. Hvam, K.A. Howard, Albumin-based drug delivery: harnessing nature to cure disease, Mol. Cell. Ther. 4 (2016) 1–12. doi:10.1186/s40591-016-0048-8.
[120] S. Jalili-Firoozinezhadi, S. Rajabi-Zeleti, P. Mohammadi, E. Gaudiello, S. Bonakdar, M.

Solati-Hashjin, A. Marsano, N. Aghdami, A. Scherberich, H. Baharvand, I. Martin, Facile fabrication of egg white macroporous sponges for tissue regeneration., Adv. Healthc. Mater. 4 (2015) 2281–2290.
[121] S. Fleischer, A. Shapira, O. Regev, N. Nseir, E. Zussman, T. Dvir, Albumin fiber scaffolds for engineering functional cardiac tissues, Biotechnol. Bioeng. 111 (2014) 1246–1257. doi:10.1002/bit.25185.
[122] P.S. Li, I. -Liang Lee, W.L. Yu, J.S. Sun, W.N. Jane, H.H. Shen, A novel albumin-based tissue scaffold for autogenic tissue engineering applications, Sci. Rep. 4 (2014) 1–7. doi:10.1038/srep05600.
[123] Q. Chang, M.A. Darabi, Y. Liu, Y. He, W. Zhong, K. Mequanin, B. Li, F. Lu, M.M.Q. Xing, Hydrogels from natural egg white with extraordinary stretchability, direct-writing 3D printability and self-healing for fabrication of electronic sensors and actuators, J. Mater. Chem. A. 7 (2019) 24626–24640. doi:10.1039/c9ta06233e.
[124] T. Schulzki, K. Seidel, H. Storch, H. Karges, S. Kiessig, S. Schneider, U. Taborski, K. Wolter, D. Steppat, E. Behm, M. Zeisner, P. Hellstern, A prospective multicentre study on the safety of long-term intensive plasmapheresis in donors (SIPLA), Vox Sang. 91 (2006) 162–173. doi:10.1111/j.1423-0410.2006.00794.x.
[125] B.A. Kaipparettu, I. Kuiatse, B.T.Y. Chan, M.B. Kaipparettu, A. V Lee, S. Oesterreich, Novel egg white - based 3-D cell culture system, Biotechniques. 45 (2008) 165–171. doi:10.2144/000112883.
[126] Z. Guo, T. Zhang, X. Chen, K. Fang, M. Hou, N. Gu, The effects of porosity and stiffness of genipin cross-linked egg white simulating aged extracellular matrix on proliferation and aggregation of ovarian cancer cells, Colloids Surfaces A Physicochem. Eng. Asp. 520 (2017) 649–660. doi:10.1016/j.colsurfa.2017.02.031.
[127] H.T. Aiyelabegan, S.S.Z. Zaidi, S. Fanuel, A. Eatemadi, M.T.K. Ebadi, E. Sadroddiny, Albumin-based biomaterial for lung tissue engineering applications, Int. J. Polym. Mater. Polym. Biomater. 65 (2016) 853–861. doi:10.1080/00914037.2016.1180610.
[128] C.C. Hsu, A. Serio, N. Amdursky, C. Besnard, M.M. Stevens, Fabrication of hemin-doped serum albumin-based fibrous scaffolds for neural tissue engineering applications, ACS Appl. Mater. Interfaces. 10 (2018) 5305–5317. doi:10.1021/acsami.7b18179.
[129] N. Nseir, O. Regev, T. Kaully, J. Blumenthal, S. Levenberg, E. Zussman, Biodegradable scaffold fabricated of electrospun albumin fibers: mechanical and biological characterization, Tissue Eng. Part C Methods. 19 (2013) 257–64.
[130] N. Amdursky, M.M. Mazo, M.R. Thomas, E.J. Humphrey, J.L. Puetzer, J.P. St-Pierre, S.C. Skaalure, R.M. Richardson, C.M. Terracciano, M.M. Stevens, Elastic serum-albumin based hydrogels: Mechanism of formation and application in cardiac tissue engineering, J. Mater. Chem. B. 6 (2018) 5604–5612. doi:10.1039/c8tb01014e.
[131] D.F. Chao, Hung-Hsing ; Torchiana, BioGlue: Albumin/glutaraldehyde sealant in cardiac surgery, J. Card. Surg. 18 (2003) 500–503. doi:10.1046/j.0886-0440.2003.00304.x.
[132] S.R. Gundry, K. Black, H. Izutani, Sutureless coronary artery bypass with biologic glued anastomoses: Preliminary in vivo and in vitro results, J. Thorac. Cardiovasc. Surg. 120 (2000) 473–477. doi:10.1067/mtc.2000.108596.
[133] F. Kratz, Albumin as a drug carrier: Design of prodrugs, drug conjugates and nanoparticles, J. Control. Release. 132 (2008) 171–183. doi:10.1016/j.jconrel.2008.05.010.
[134] D. Sleep, Albumin and its application in drug delivery, Expert Opin. Drug Deliv. 12

(2015) 793–812. doi:10.1517/17425247.2015.993313.
[135] A. Gaspar, L. Moldovan, D. Constantin, A.M. Stanciuc, P.M. Sarbu Boeti, I.C. Efrimescu, Collagen-based scaffolds for skin tissue engineering., J. Med. Life. 4 (2011) 172–177.
[136] V.G. Arzumanyan, I.M. Ozhovan, O.A. Svitich, Antimicrobial effect of albumin on bacteria and yeast cells, Bull. Exp. Biol. Med. 167 (2019) 763–766. doi:10.1007/s10517-019-04618-6.
[137] E.A. Charter, G. Lagarde, Encyclopedia of food microbiology (Second edition), Elsevier Ltd., 2014.
[138] A. Blaeser, D.F. Duarte Campos, U. Puster, W. Richtering, M.M. Stevens, H. Fischer, Controlling shear stress in 3D bioprinting is a key factor to balance printing resolution and stem cell integrity, Adv. Healthc. Mater. 5 (2016) 326–333. doi:10.1002/adhm.201500677.
[139] J.P.E. Junker, R.A. Kamel, E.J. Caterson, E. Eriksson, Clinical impact upon wound healing and inflammation in moist, wet, and dry environments, Adv. Wound Care. 2 (2013) 348–356. doi:10.1089/wound.2012.0412.
[140] P. Escobar, S. Wittles, S. Asfour, L. Latta, Mechanical characteristics of muscle, skin and fat-elastic moduli for finite element modeling of limbs, 19th Int. Tech. Conf. Enhanc. Saf. Veh. (2005) 4. http://www-nrd.nhtsa.dot.gov/pdf/nrd-01/esv/esv19/05-0250-O.pdf.
[141] N. Momtahan, N. Poornejad, J.A. Struk, A.A. Castleton, B.J. Herrod, B.R. Vance, J.P. Eatough, B.L. Roeder, P.R. Reynolds, A.D. Cook, Automation of pressure control improves whole porcine heart decellularization, Tissue Eng. - Part C Methods. 21 (2015) 1148–1161. doi:10.1089/ten.tec.2014.0709.
[142] H.A. Mansy, J.R. Grahe, R.H. Sandler, Elastic properties of synthetic materials for soft tissue modeling, Phys. Med. Biol. 53 (2008) 2115–2130. doi:10.1088/0031-9155/53/8/008.
[143] V. Uskoković, S. Ghosh, Carriers for the tunable release of therapeutics: etymological classification and examples, Expert Opin. Drug Deliv. 13 (2016) 1729–1741. doi:10.1080/17425247.2016.1200558.
[144] C.S. Chamberlain, E. Crowley, R. Vanderby, The spatio-temporal dynamics of ligament healing, Wound Repair Regen. 17 (2009) 206–215. doi:10.1111/j.1524-475X.2009.00465.x.
[145] M. Mendoza García, M. Izadifar, X. Chen, Evaluation of PBS treatment and PEI coating effects on surface morphology and cellular response of 3D-printed alginate scaffolds, J. Funct. Biomater. 8 (2017) 48. doi:10.3390/jfb8040048.
[146] C.M. Agrawal, J.S. McKinney, D. Lanctot, K.A. Athanasiou, Effects of fluid flow on the in vitro degradation kinetics of biodegradable scaffolds for tissue engineering, Biomaterials. 21 (2000) 2443–2452. doi:10.1016/S0142-9612(00)00112-5.
[147] J.A. Reid, A. Callanan, Hybrid cardiovascular sourced extracellular matrix scaffolds as possible platforms for vascular tissue engineering, J. Biomed. Mater. Res. - Part B Appl. Biomater. 108 (2020) 910–924. doi:10.1002/jbm.b.34444.
[148] D.F. Williams, The Williams dictionary of biomaterials, Liverpool University Press, 1999.
[149] J.M. Anderson, G. Cook, B. Costerton, S.R. Hanson, A. Hensten-Pettersen, N. Jacobsen, R.J. Johnson, R.M. Mitchell, M. Pasmore, F. Schoen, M. Shirtliff, P. Stoodley, Host reactions to biomaterials and their evaluation, in: Biomater. Sci., 1996: pp. 165–214. doi:10.1016/b978-0-08-050014-0.50009-2.
[150] N. Soltan, L. Ning, F. Mohabatpour, P. Papagerakis, X. Chen, Printability and cell

viability in bioprinting alginate dialdehyde-gelatin scaffolds, ACS Biomater. Sci. Eng. 5 (2019) 2976–2987. doi:10.1021/acsbiomaterials.9b00167.

Appendices

Appendix I

Rheological curves of shear stress versus shear rate for each prepared EW-Alg blend.

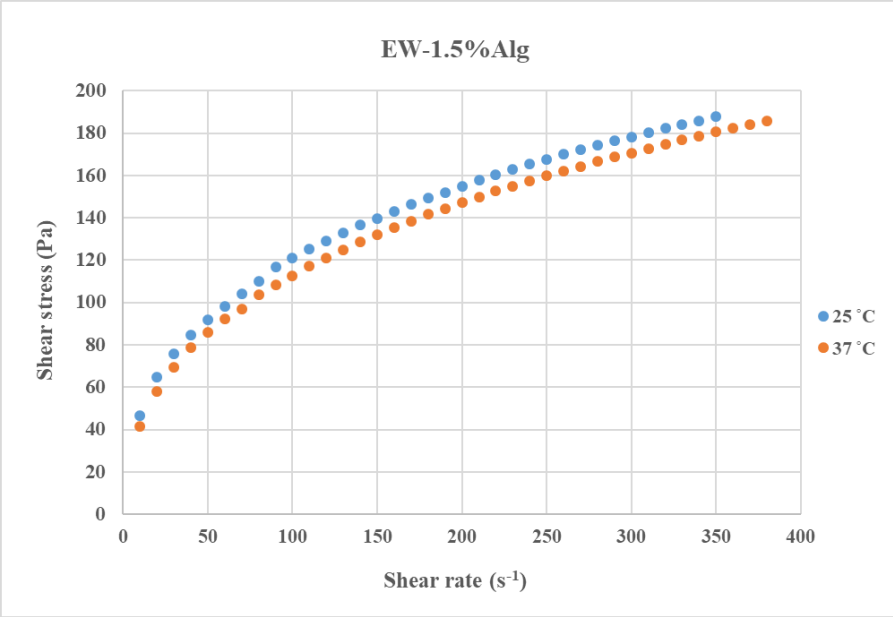

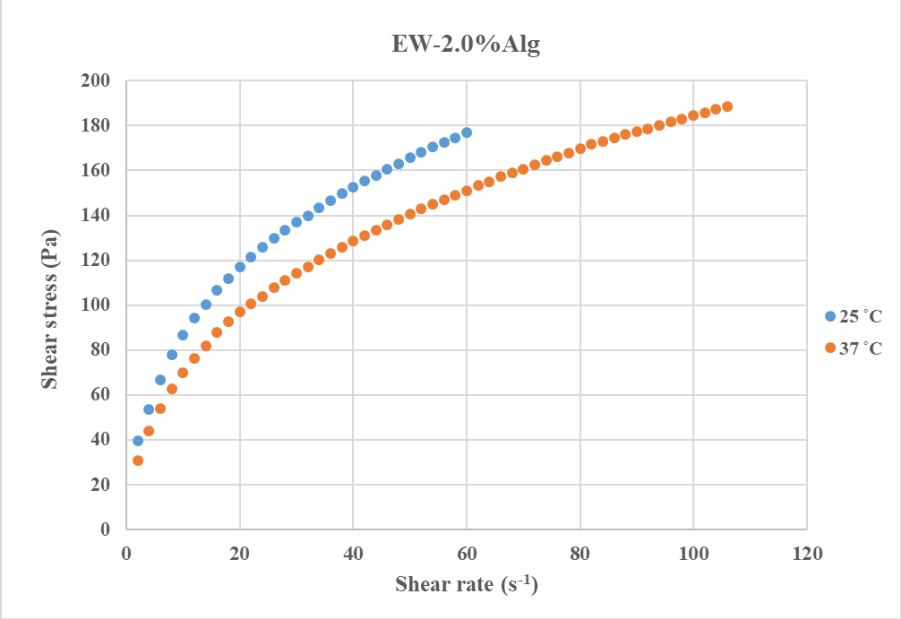

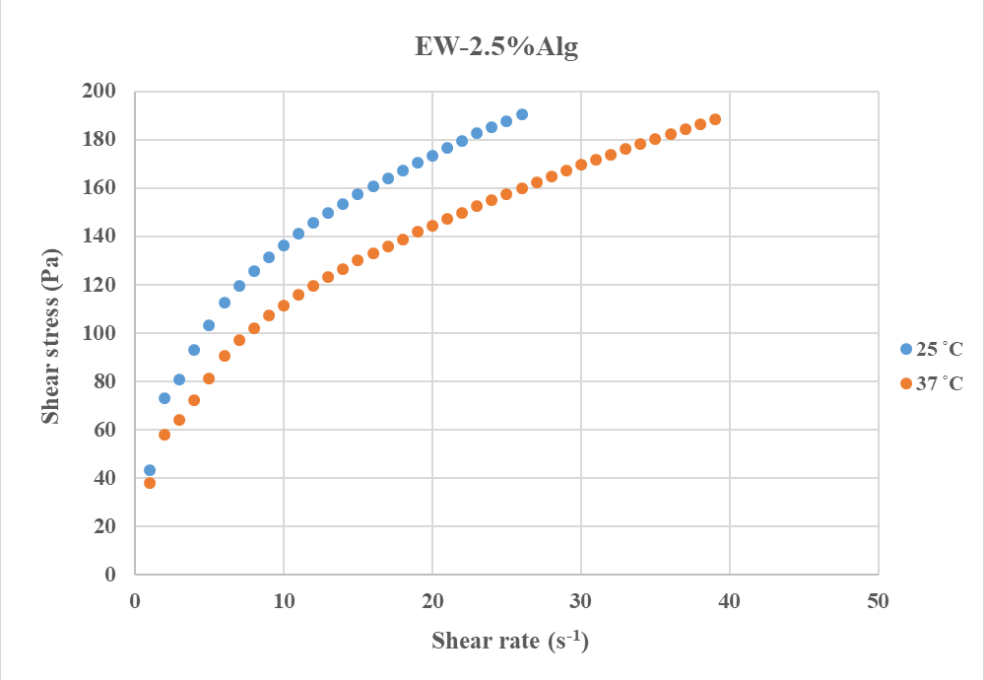
EW-2.5%Alg
Shear stress (Pa)
Shear rate (s-1)
0
20
40
60
80
100
120
140
160
180
200
0
10
20
30
40
50
25 ˚C
37 ˚C

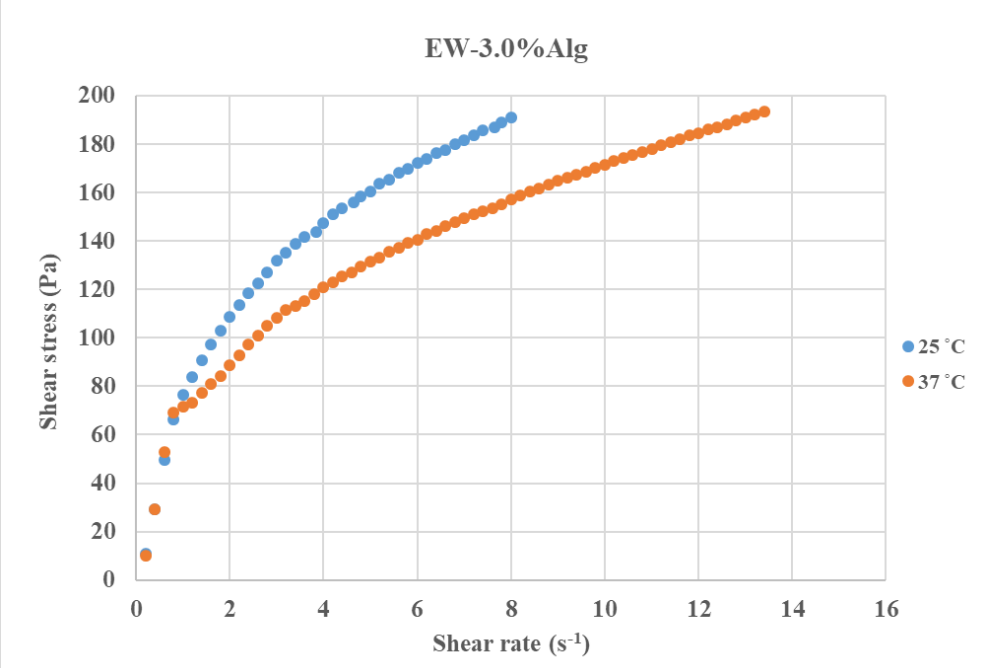
EW-3.0%Alg
Shear stress (Pa)
Shear rate (s-1)
0
20
40
60
80
100
120
140
160
180
200
0
2
4
6
8
10
12
14
16
25 ˚C
37 ˚C

Appendix II

Compressive elastic properties of synthetic materials for soft tissue modeling [142].

No.	Material, manufacturer, city, state	Density (g ml^{-1})	Softener volume range[a](%)	Modulus range[a] (kPa)	Approximate cost per gallon
1	SR-1610, Douglas and Sturgess, San Francisco, CA	1.15	0–58[b]	25–660	$100
2	Dragon skin, Smooth-On, Easton, PA	1.08	0–78[b]	20–850	$85
3	Ecoflex 00-10, Smooth-On, Easton, PA	1.03	0–50[b]	15–110	$105
4	HS-IV, Dow Corning, Midland, MI	1.11	0–48[b]	20–570	$140
5	Candle Gel, Endless Possibilities, Oklahoma City, OK	0.98	n/a	50	$35
6	Tin-Sil, US Composites, West Palm Beach, FL	1.07	0–82[b]	10–1400	$200
7	Semicosil 921, Wacker Solutions, Adrian, MI	1.10	n/a	25	$110
8	8116SS plastic, M-F Manufacturing, Ft. Worth, TX	0.99	0–56[c]	15–200	$40
9	CF11, Nusil Technologies, Carpinteria, CA	1.04	n/a	204	$240

[a]covers the softener volume range where specimens can cure.
[b]uses MC-1155 silicone fluid (Douglas and Sturgess, San Francisco, CA) as a softener.
[c]uses 4116S Plastic Softener (M-F Manufacturing, Ft. Worth, TX) as a softener.

Appendix III

a) Efforts to 3D print constructs made of EW 40%w + Sugar (glucose) 60%w solution (meringue).

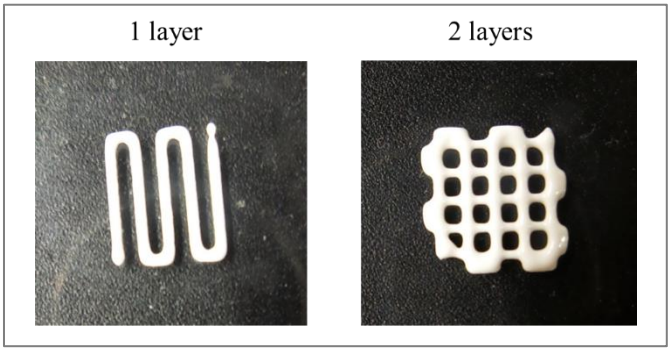

b) Efforts to 3D print constructs made of EW 80%w + Gelatin 20%w.

Appendix IV

Heated form of EW-2.0%Alg after autoclaving. Porous bulk (left), extruded form within the $CaCl_2$ 25mM bath (right).